

Seismic response characteristics of concentrically K-braced steel structures

Hiroyuki Yamanouchi & Toshibumi Fukuta

Building Research Institute, Ministry of Construction, Government of Japan (BRI)

ABSTRACT: Seismic performance of concentrically K-braced steel building structures is studied by parametric dynamic response analysis with a hysteresis model of K-braced structures, which was verified by the experimental results on a six-story full-scale building and scale-model frames with three-story. These studies provide an useful design flow and some charts resolving important problems on the K-braced system.

1 INTRODUCTION

Although concentrically K-braced steel building structures have been widely used as an earthquake resistant structural system, appropriate information on how to design the system effectively is yet insufficient.

This is due to the lack of knowledge on (1) the interaction between the brace and the surrounding frame, in particular, the girder in braced bay and (2) proportioning of the seismic load and deformation capacity to the K-braces and the moment-resisting frames.

This paper deals with the above two problems and leads to some recommendations for design of the K-braced structure with intermediate slenderness of braces ($L/i=70-120$), which are often designed as seismic elements of middle-rise buildings.

Namely, the first problem is dealt in discussion by using the experimental and analytical results on the K-braced system.

The second problem is studied parametrically by dynamic response analyses involving the effect of the brace-to-girder interaction considered in the first problem. Here, to avoid the increase of the number of parameters for analysis and to attain general knowledge for design, a simple analytical model of lumped mass system is developed.

The analytical results make a design flow with several charts suggestive to designers, emphasizing the effect of the interaction of seismic characteristics between K-braced bay and the rest frame portion on the response characteristics of the whole system.

2 A SIMPLIFIED HYSTERESIS MODEL OF K-BRACED STRUCTURAL SYSTEM

A planar frame with the concentrically K-braced bay can be decomposed into the two sub-structures, as is schematically shown in Fig.1.

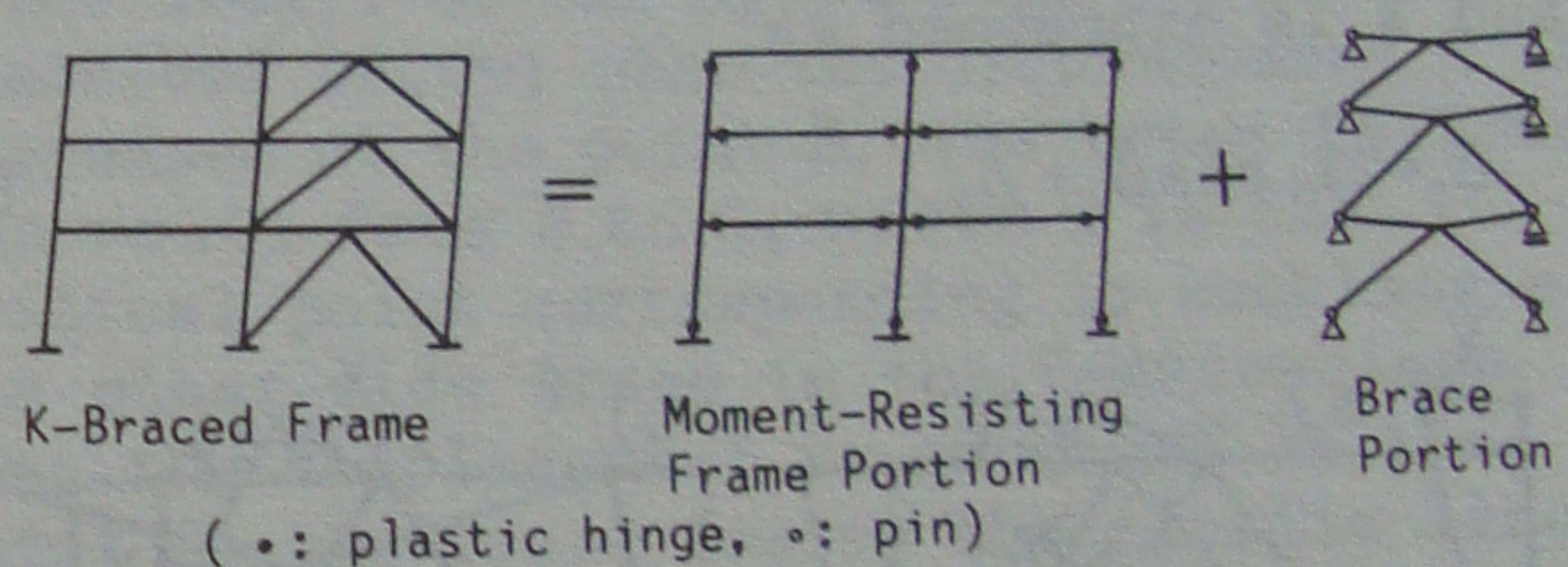


Fig.1 Decomposition into Two Sub-Structures

Here assuming that the stress redistribution between the sub-structural portions after yielding is negligible and each structural portion exhibits resisting story shear independently for the same inter-story displacement X , the shear force of a story is given by Eq.1.

$$Q(X) = Q_f(X) + Q_b(X) \quad (1)$$

where $Q_f(X)$ is the story shear carried by the moment-resisting frame portion and $Q_b(X)$ is the story shear carried by the K-brace portion.

2.1 $Q_f(X)$ of Moment-Resisting Frame Portion

$Q_f(X)$ - X relation of the moment-resisting frame portion was assumed to be under the bi-linear and perfect elasto-plastic

hysteresis rule.

2.2 Q(X) of Compression-Side Brace

$Q_b(X)$ was assumed to be the sum of the story shear carried by a pair of compression- and tension-side braces. $Q(X)$ - X relation of the compression-side brace was completed as follows: in the region before the buckling, the relations in the compression-side brace among axial force P , axial displacement Δ_2 and X are expressed as

$$\begin{aligned} P(\Delta_2) &= K_{br} \Delta_2, \quad \Delta_2 = X \cos \theta \\ Q_{bc}(X) &= P(\Delta_2) \cos \theta = K_b X \end{aligned} \quad (2)$$

where K_{br} is the axial elastic stiffness and K_b is the elastic story-stiffness of the brace. Thus, modifying the equation,

$$K_b = K_{br} \cos^2 \theta \quad (3)$$

After buckling of the compression-side brace, the downward pulling force at the brace-to-girder junction point, caused by the unbalanced force between the tension- and compression-side braces, results in the downward vertical displacement at the mid-span of the girder. In this case, referring to Fig.2.b, the relation among Δ and X is expressed as

$$\Delta_2 = 2X \cos \theta + \Delta_1 \quad (4)$$

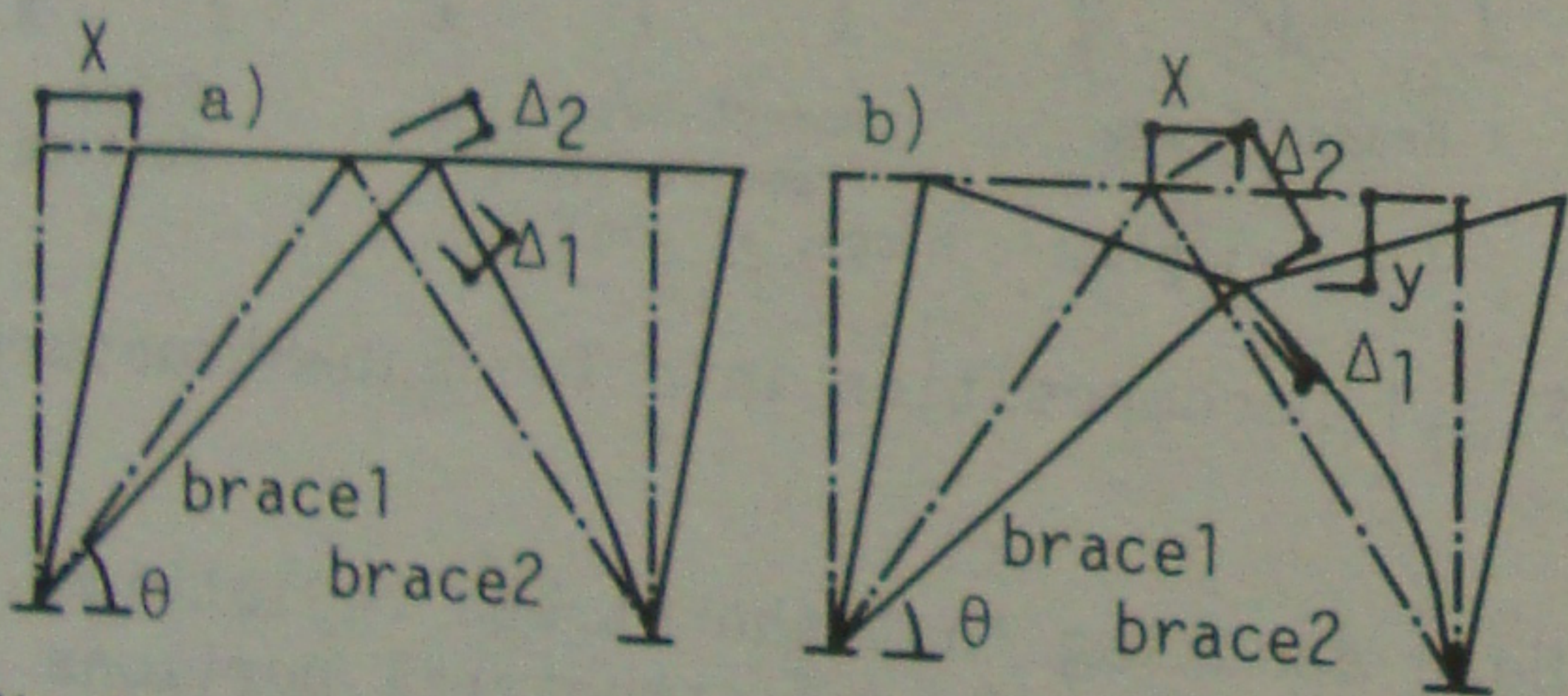


Fig.2 Compatibility of Deflection of Braces

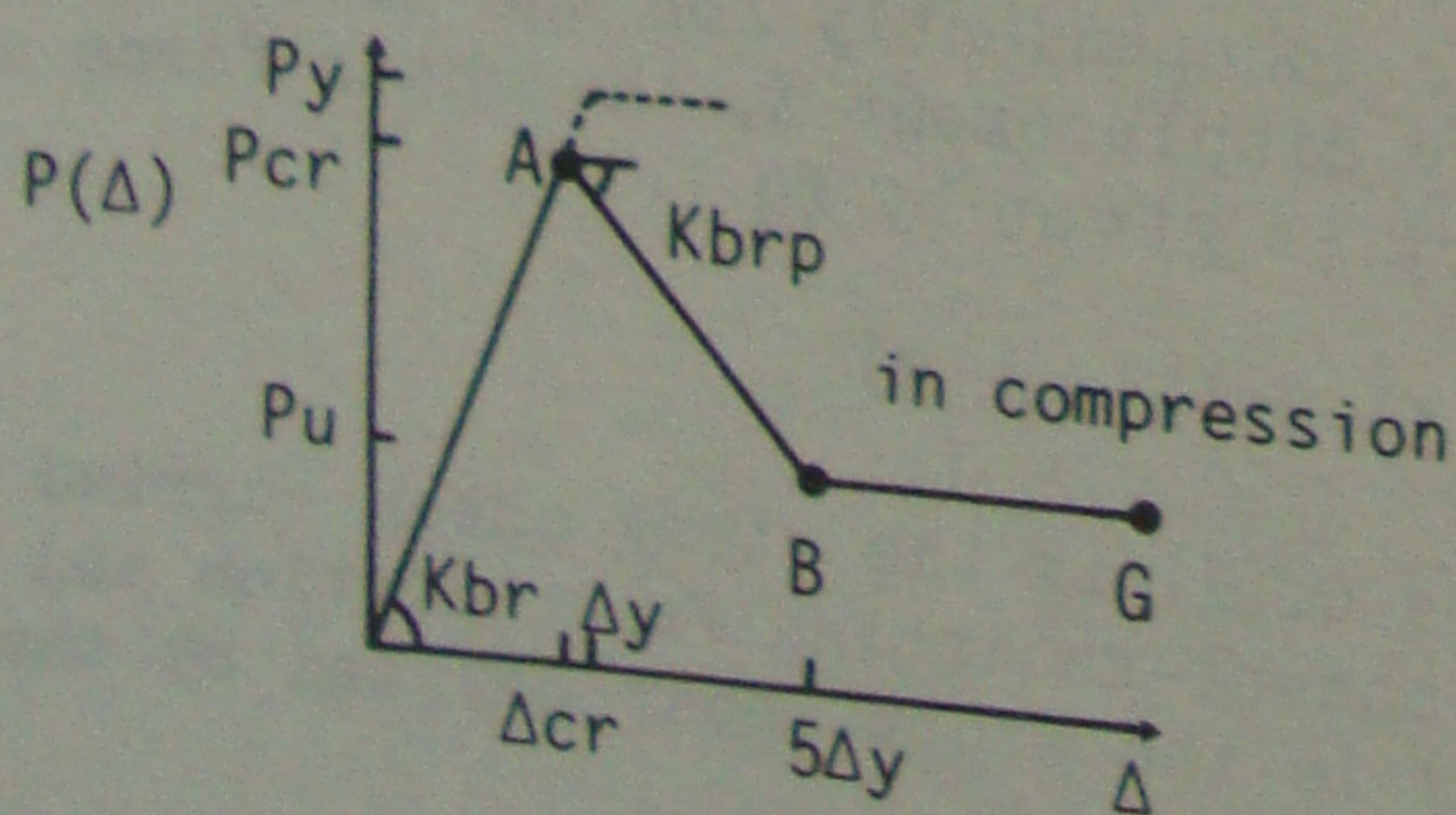


Fig.3 P- Δ Relation of Braces

As the resisting force of the compression-side brace decreases after the buckling, the tension-side brace is correspondingly

unloaded elastically and decreases its axial displacement. Yet, the decrement of the axial displacement in the latter brace is neglected, because the decrement is very small. The axial force-axial displacement relations (P - Δ relations) of the braces in the post-buckling range were approximated by two straight line as shown in Fig.3.

Thus, the post-buckling relations for the compression-side brace among P , $Q(X)$, Δ_2 , and X are obtained as the incremental expression.

$$\begin{aligned} dP(\Delta_2) &= K_{brp} d\Delta_2 \\ dQ_{bc}(X) &= dP(\Delta_2) \cos \theta = K_{bp} dX \\ d\Delta_2 &= 2dX \cos \theta + d\Delta_1 = 2dX \cos \theta \\ K_{bp} &= 2K_{brp} \cos^2 \theta \end{aligned} \quad (5)$$

where K_{brp} is the descending slope in the P - Δ relation, K_{bp} is the descending slope in the $Q(X)$ - X relation and $Q_{bc}(X)$ is the story shear carried by the compression-side brace (Fig.4).

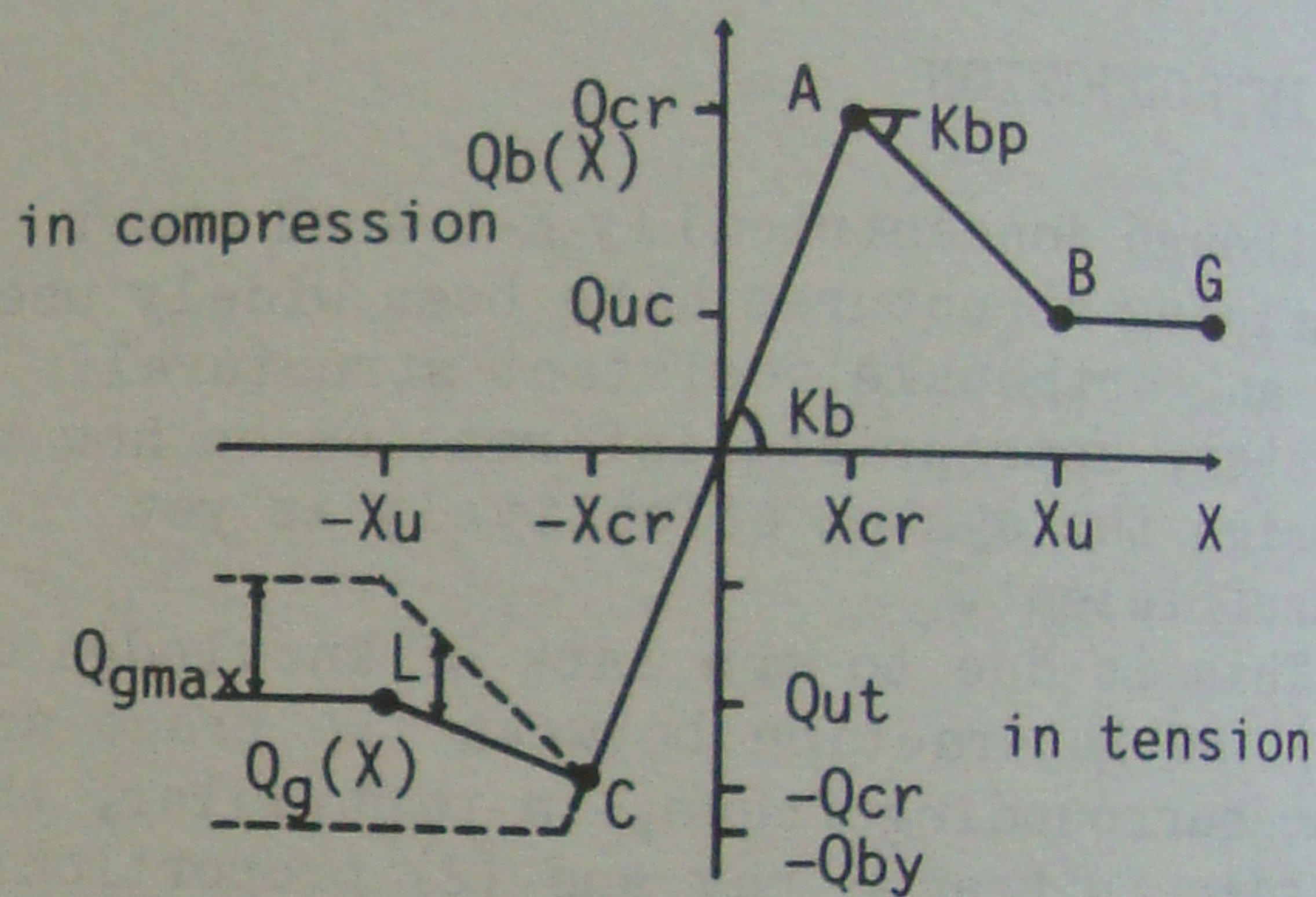


Fig.4 $Q_b(X)$ - X Relation of Braces

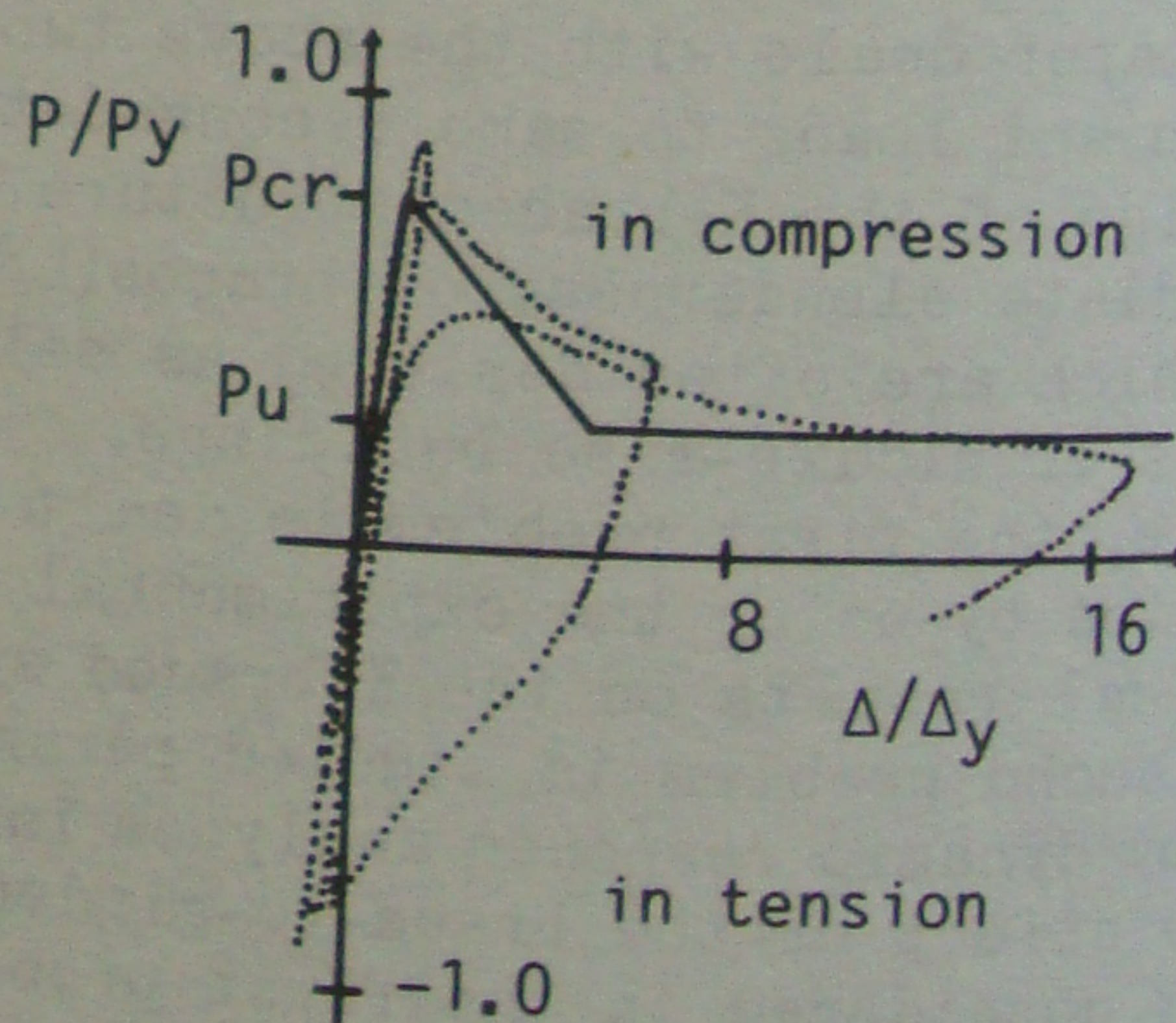


Fig.5 Comparison of P - Δ relation between test and proposed analytical results

Q_{uc} in Fig.4 was formulated on the basis of the theoretical analysis and experiment about the elastically end-restrained brace. The braces in K-braced frames are generally restrained at their ends by surrounding members such as columns and girders. The work of the authors (1986) found that the

post-buckling P-Δ relation of the compression member with K-factor for the buckling >0.5 is very close to that of a pin-supported member with the identical section and the length of a half of the former one's. Adopting this findings, Q_{uc} was formulated as follows:

$$Q_{uc} = P_u \cos\theta = P_y (0.5 - 0.065\lambda_e) \cos\theta \quad (6)$$

where P_y is the yield axial force and using the yield strain ϵ_y , λ_e is defined as $\lambda_e = \sqrt{\epsilon_y L}/i$. The descending slope K_{brp} was determined in consideration of the above analytical results and experiment (Fig.3). In Fig.5, good agreement is shown on P-Δ relations for both the experimental and proposed analytical results.

2.3 Q(X) of Tension-Side Brace

The shear force carried by the tension-side brace $Q_{bt}(X)$ can be given after the buckling of the compression-side brace as the sum of the shear force $Q_{bc}(X)$ in the compression-side brace and the shear force $Q_g(X)$ that is specified as the brace-to-girder interaction, by the contribution of the girder in the K-braced bay.

Here, the amount of $Q_g(X)$ is assumed to increase linearly from the point C where corresponds to the occurrence of the buckling in compression-side brace up to the point L, resulting in the constant value Q_{gmax} after the point L (Figs. 4 and 6). This feature of $Q_g(X)$ is analyzed for the several combinations among braces, columns and girders. As a result, $Q_{bt}(X)$ is expressed as follows:

$$Q_{bt}(X) = -Q_{bc}(X) - Q_g(X), \quad Q_{bt}(X) < P_y \cos\theta \quad (7)$$

From the above discussions, the final Q(X)-X relation of the brace has been obtained as shown in Fig.4.

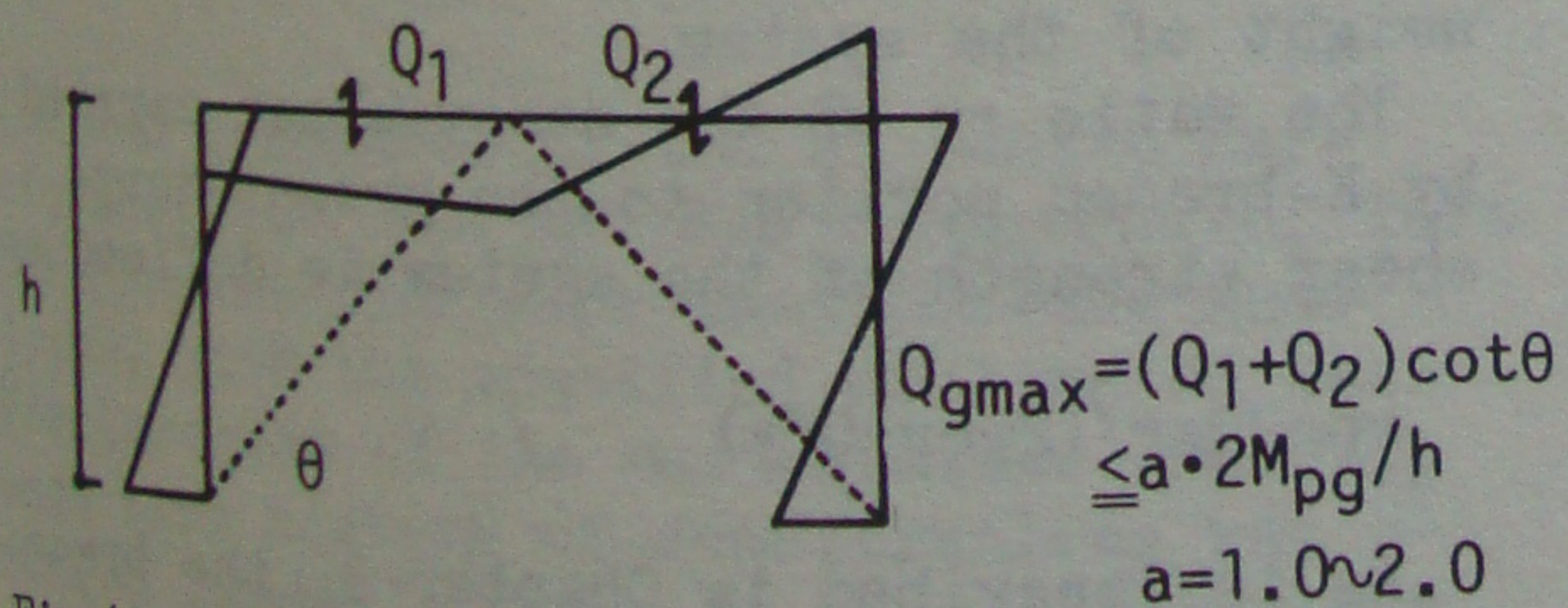


Fig.6 Contribution of Girders to Shear Force

2.4 Proposed Hysteretic Model of Brace

In the foregoing discussion, the Q(X)-X relation of the brace under the monotonic story-displacement were derived from the P-Δ relations of the brace. Now, on the basis

of these results, the hysteretic Q(X)-X relation of the brace under cyclic and reversed loadings is developed to conduct dynamic response analyses on the K-braced system.

The representative hysteretic Q(X)-X relation of one-side brace of the K-assembly constructed by the rules are schematically shown in Fig.7, for a specified history of story drift X which provides all possible behavior of the brace from the point A to Q in alphabetical order.

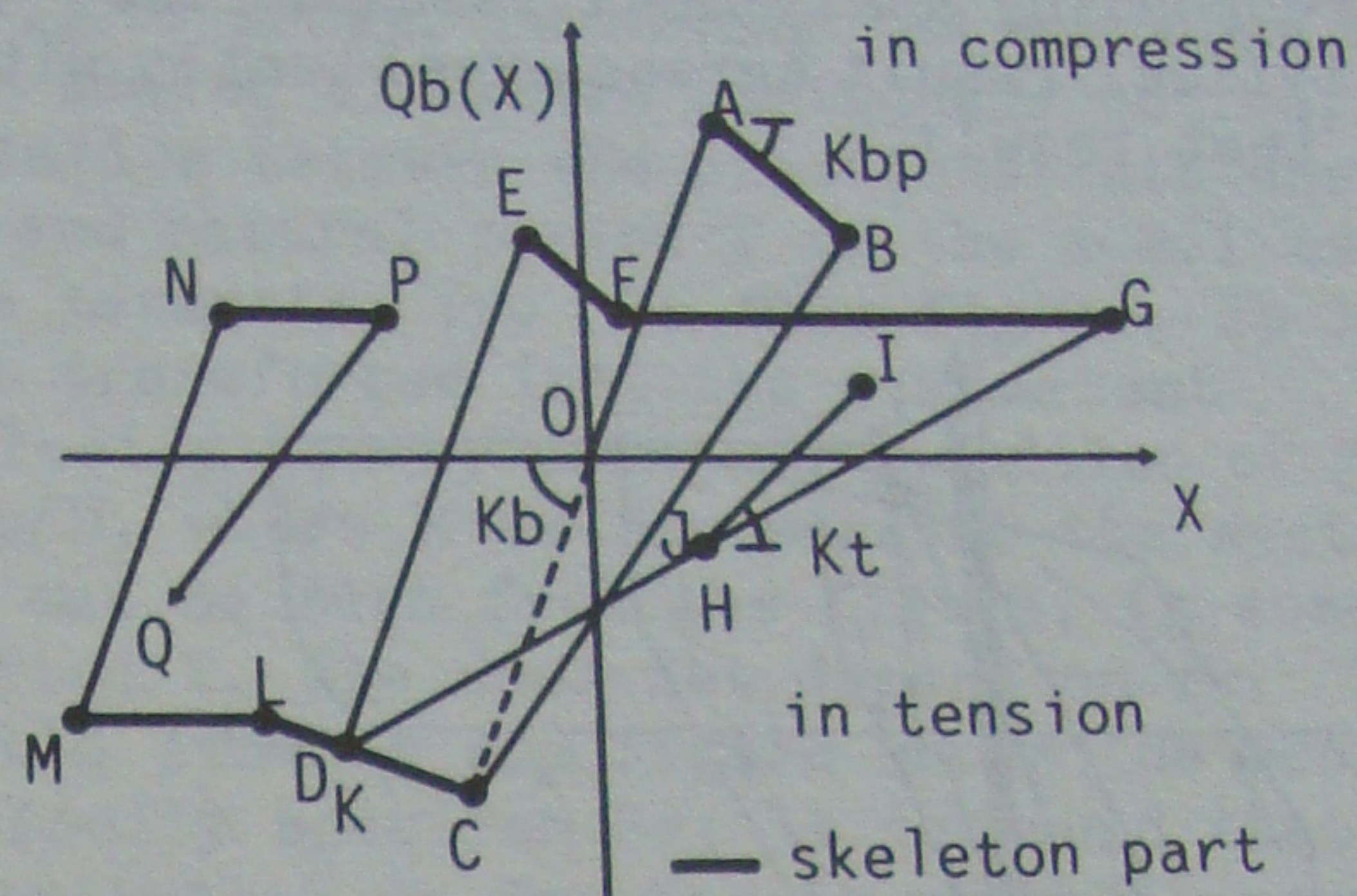


Fig.7 Hysteretic Rule of Braces

The detail of the hysteretic model is described below; when the displacement X is decreased at the point B, the brace follows the route from B to C, where C is the critical point corresponding to buckling of the other-side brace in the K-assembly. When the displacement is reversed at the point D, the brace traces the elastic line from D to E with the slope K_b . At the point E, where force level is equal to that of point B, the brace begins to detract in the load-capacity to the level of point F. Here, the lines AB, EF and FG are corresponding to the skeleton line ABG in Fig.4. When the displacement reversed at the point G, the brace goes to the point D which is corresponding to the maximum displacement experienced in the past cycles, on the tension-side skeleton lines CLM. When the displacement increases after reaching to the point D, the part of the skeleton lines, DLM are followed. Moreover, returning to the line GD, when the displacement is reversed positive from the point H, the line HI with the slope K_t is traced, where K_t is given empirically as $K_t = 2K_b K_c / (K_b + K_c)$.

2.5 Verification of Proposed Hysteresis Model by Test Results

The hysteresis model for K-braced systems

was applied to our test results on one of the half-scaled K-braced frames(1984) and the full-scale six-story K-braced building (1984) in order to obtain the validity of the hysteresis model. For the analysis of the former test, the displacement history given in the test was used to predict the Q(X)-X relation by the proposed model. The later test results(by the pseudo-dynamic test technique) were compared with those of response analysis using the hysteresis model.

Fig.8 shows the Q(X)-X relations for both the half-scaled model frame and the corresponding analytical result. The analytical result agrees excellently with the test result.

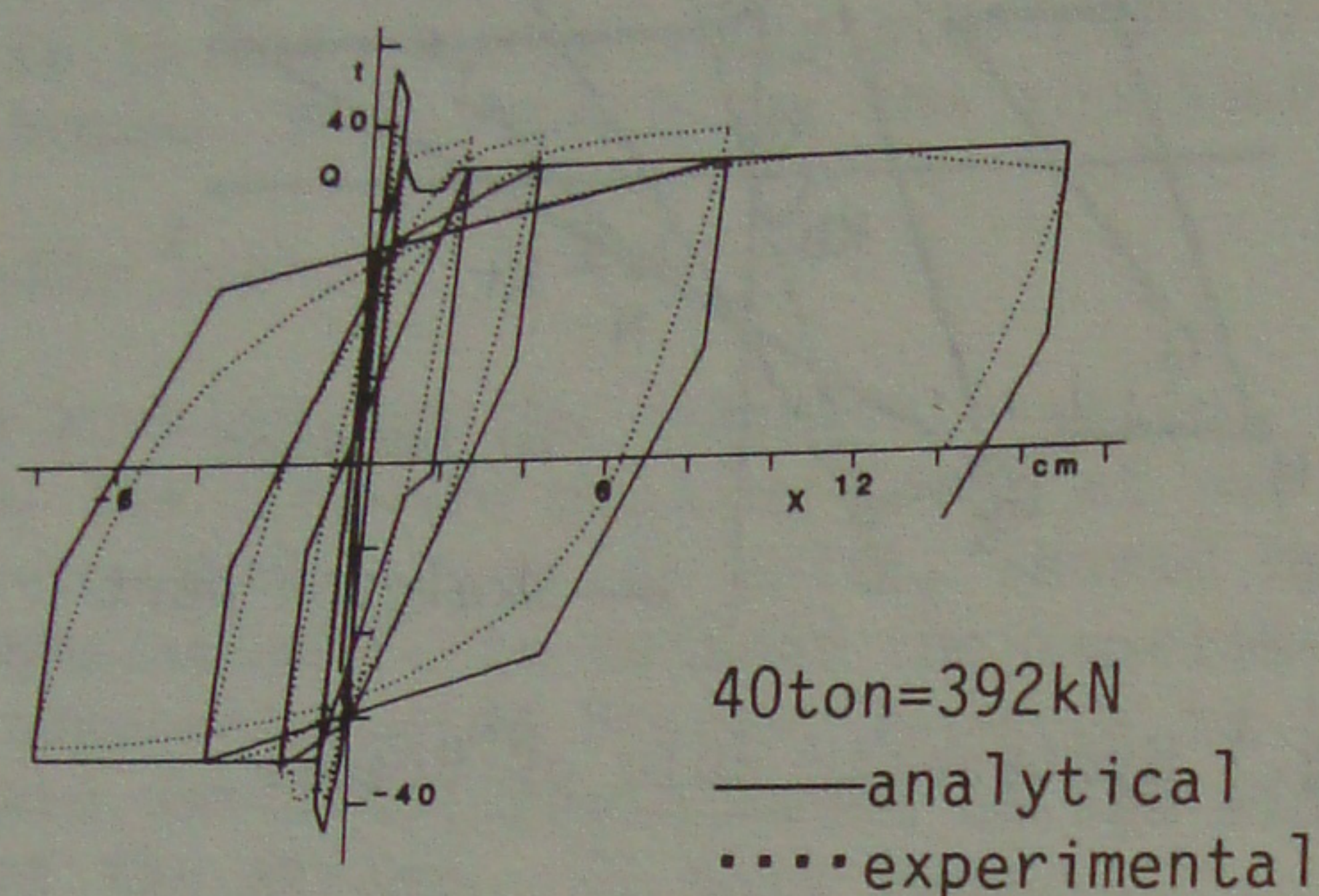


Fig.8 Comparison between Experimental and Analytical Q(X)-X Relation of Half-Scaled K-Braced Frame

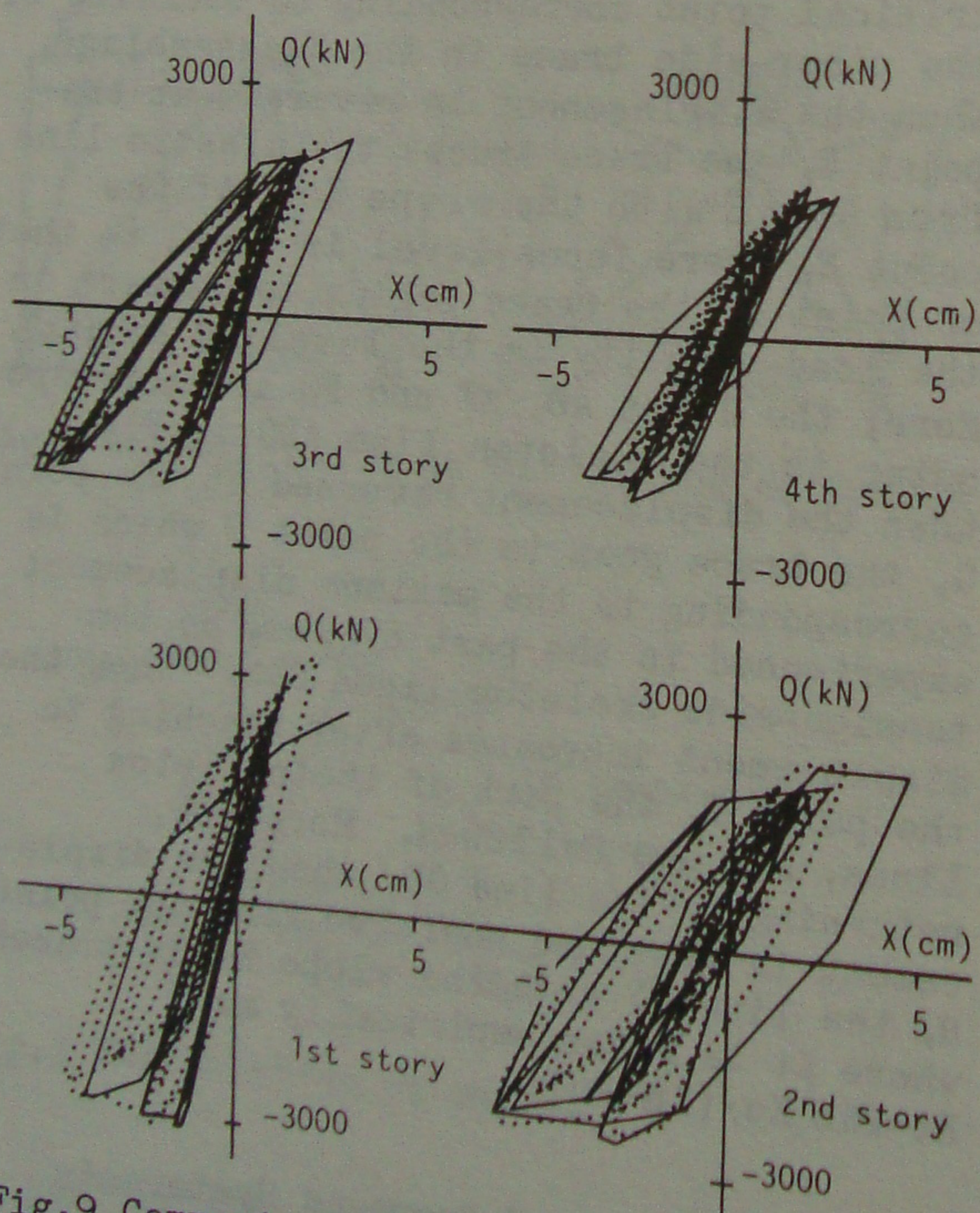


Fig.9 Comparison between Experimental and Analytical Q(X)-X Relation of Full-Scale Six-Story K-Braced Building

As for the full-scale test, Fig.9 shows the Q(X)-X relation for the lower four stories. Also from the figure, good agreement can be found between the experimental and analytical results. Accordingly, it can be said that the hysteresis model for the K-braced system proposed in this paper has much verification, whereas it is so much simple.

3 PARAMETRIC RESPONSE ANALYSES

This chapter, first, deals with parametric dynamic response analyses on one-degree-of-freedom of lumped mass systems with the hysteresis model discussed above. Second, response results are examined by the content on the plastic-strain-energy absorbed in the system. For these systems, the major response characteristics of the energy are extracted, in particular for the two sub-structural portions. Third, this knowledge is confirmed by the response analyses on a three-degree-of-freedom dynamic system that would be a representative for multi-story structures having the concentration of response energy along the height of the structure.

3.1 Analytical parameters on one-degree-of-freedom system

The six basic parameters, which were strongly expected to have significant effects on the response, were carefully selected for the analyses of the K-braced system with one-degree-of-freedom.

The yield story-shear coefficient r_y of the system is defined as

$$r_y = (Q_{fy} + 2Q_{cr}) / W \quad (8)$$

where Q_{fy} is the yield story-shear of the moment-resisting frame portion, Q_{cr} is the story-shear at the buckling of one-side brace of the K-braced portion and W is the weight of the system.

The ratio r_p of the story-shear carried by K-braced portion to the gross story-shear strength of the system is defined as

$$r_p = 2Q_{cr} / (2Q_{cr} + Q_{fy}) \quad (9)$$

As is described in Chapter 3, the brace-to-girder interaction in the K-braced bay can be represented by $Q_g(X)$; $Q_g(X)$ has the maximum value of Q_{gmax} (Fig.4). Namely, the resisting shear force $Q_{bt}(X)$ in the tension-side brace increases by $Q_g(X)$, at the maximum by Q_{gmax} , as a result of the contribution of the girder to the shear capacity of the K-braced bay. Here, the degree of the girder's contribution is defined as

$$r_s = Q_{gmax} / Q_{by} \quad (10)$$

where Q_{by} is the tensile yield story-shear of the brace (Fig.4).
The elastic stiffness shared by the K-braced portion in the gross elastic stiffness of the system can be expressed by using the ratio as follows

$$r_s = 2K_b / (2K_b + K_f) \quad (11)$$

where K_f is the elastic stiffness of the moment-resisting frame portion.
The relation between r_p and r_s can be introduced by the following equations;

$$\begin{aligned} Q_{fy} &= K_f X_{fy}, \quad Q_{cr} = K_b X_{cr} \\ r_s &= C r_p / (C r_p - r_p + 1), \quad C = X_{fy} / X_{cr} \end{aligned} \quad (12)$$

In general K-braced steel structures, the range of C would be $1 < C < 6$. Therefore, the combination between r_p and r_s was adopted for the analyses considering the range of C . The other parameters are the natural period of the system and slenderness L/i of the brace. The values of the six parameters used in the analyses are listed in Table 1.

Table 1 Value of parameters used in the analyses

parameter	value
T(sec.)	0.1, 0.3, 0.6, 0.9, 1.2, 1.5, 1.8
r_y	0.15, 0.3
(r_p, r_s)	(0.0, 0.0), (0.2, 0.2), (0.2, 0.3) (0.2, 0.4), (0.2, 0.5), (0.2, 0.6) (0.4, 0.4), (0.4, 0.5), (0.4, 0.6) (0.4, 0.7), (0.4, 0.8), (0.6, 0.6) (0.6, 0.7), (0.6, 0.8), (0.6, 0.9) (0.8, 0.8), (0.8, 0.9), (0.8, 0.95) (1.0, 1.0)
r_g	0.2, 0.4, 0.6, 0.8
L/i	70, 120

The N-S component of the El Centro Earthquake (1940) and the E-W component of Taft Earthquake (1952) were used for the analyses, with the specified scaling on each accelerogram of the earthquakes. Namely, each time history of accelerations was scaled linearly so as to have the maximum velocity response spectrum of 50 cm/sec for the system with the natural period of 10 sec. and the damping ratio of $1/\sqrt{2}$. This treatment provides an anchor level of the intensity of the earthquake ground motions for the engineering-design aspects.

3.2 Examination of analytical results on one-mass system

-total plastic-strain-energy absorbed in the system- As widely recognized, the plastic-strain-energy absorbed in a structure during seismic response is a very significant index to evaluate structural damage. First of all, therefore, the characteristics of the absorbed energy were studied on the results of the above analyses. The plastic-strain-energy was computed by summing up the area of each hysteretic story shear-displacement loop induced in the analytical model during the response.

Fig.10 shows, regarding the response by the scaled El Centro Earthquake motion, the relation between the plastic-strain-energy E_p and natural period T of the model using the parameter r_s . In this figure, E_p is yet transformed into the equivalent velocity V_{pe} by using the equation of $V_{pe}^2 = 2E_p/M$, where M is the mass of the system. As can be seen from the figure, in some period T , V_{pe} does not depend on r_s . The solid line in the figure shows the response velocity spectrum S_v ; it is found that substituting S_v for V_{pe} is probably useful for design, if the information on V_{pe} is not obtained for an earthquake motion.

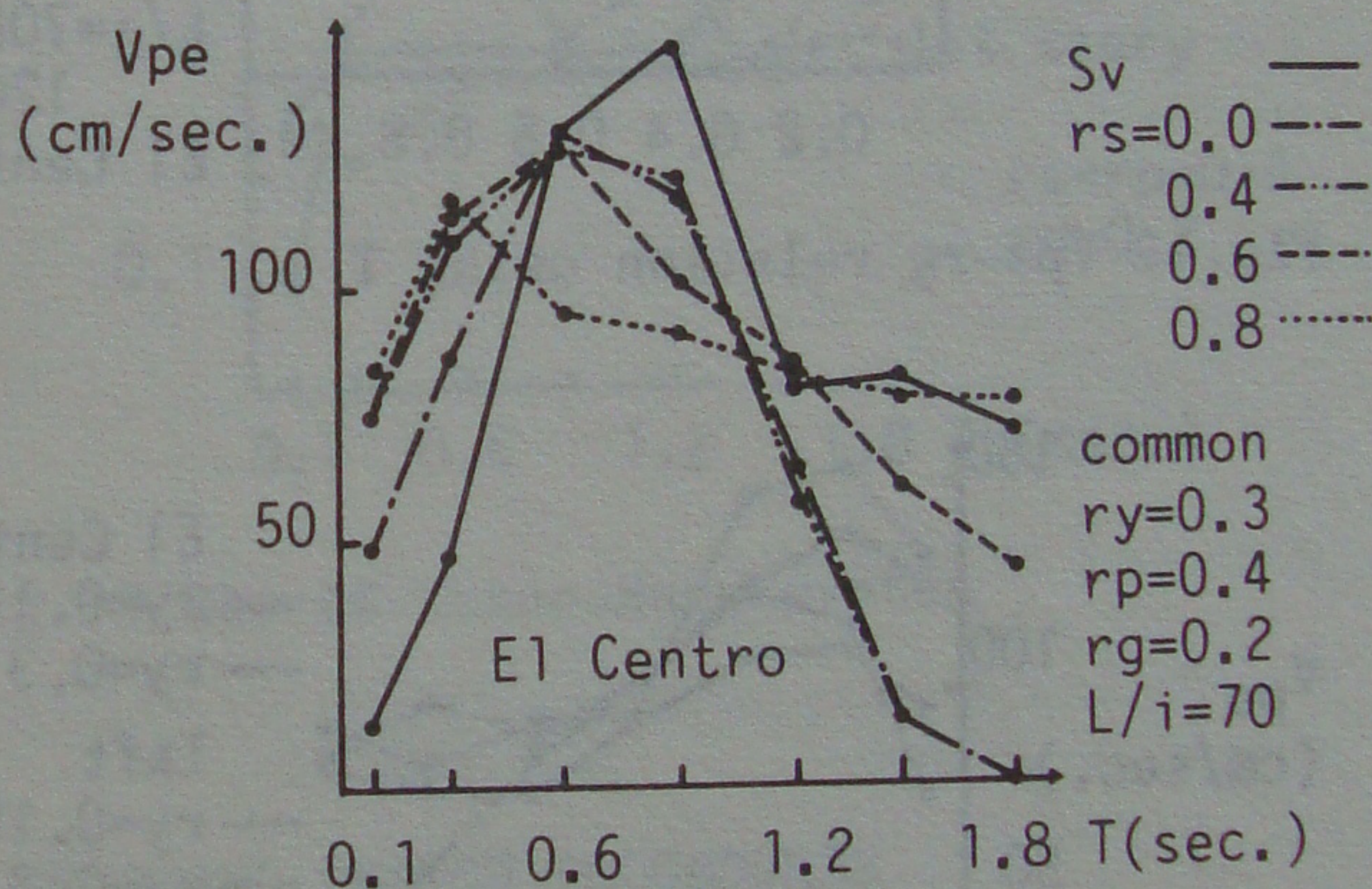


Fig.10 V_{pe} and S_v -T relation using r_s

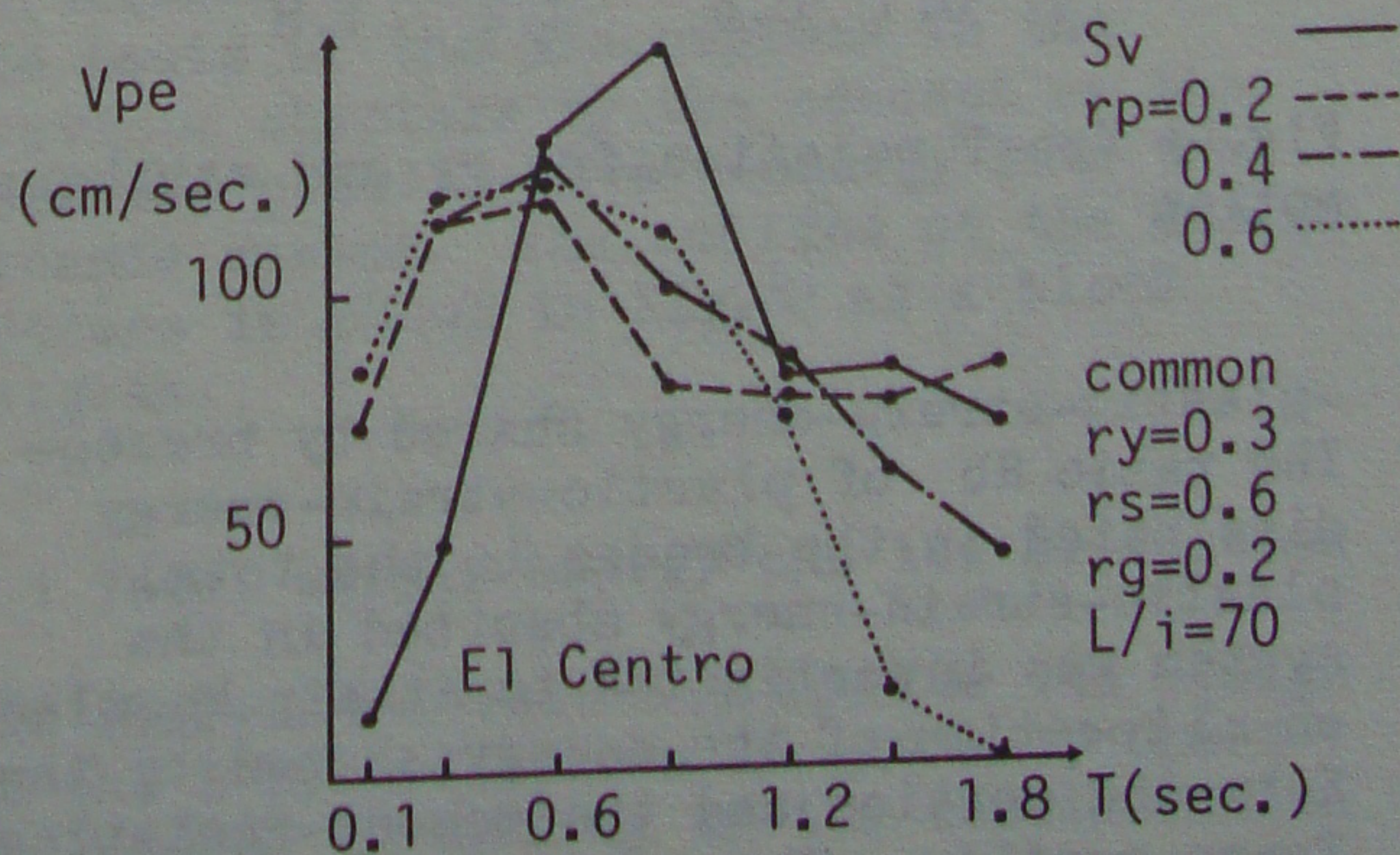


Fig.11 V_{pe} and S_v -T relation using r_p

Next, in the important parameters, r_p was examined whether it affects V_{pe} or not. Fig.11 exhibits V_{pe} as a function of T using the parameter r_p . The trend of the V_{pe} - r_p relations is found to be similar to that of the V_{pe} - r_s relations.

Also the influence of the brace-to-girder interaction coefficient r_g on V_{pe} is drawn in Fig.12, for the different slenderness $L/i=70$ and 120 . This figure shows that r_g and L/i have almost no effect on V_{pe} .

Finally for V_{pe} , the yield story-shear coefficient r_y was examined. As is visible in Fig.13 for each of the earthquake motions, the dependence of V_{pe} on T is smaller for $r_y=0.15$ than for $r_y=0.3$; obviously, the damage of the system becomes severe as r_y decreases, though a considerable difference is in the V_{pe} - r_y relation between the two earthquake motions.

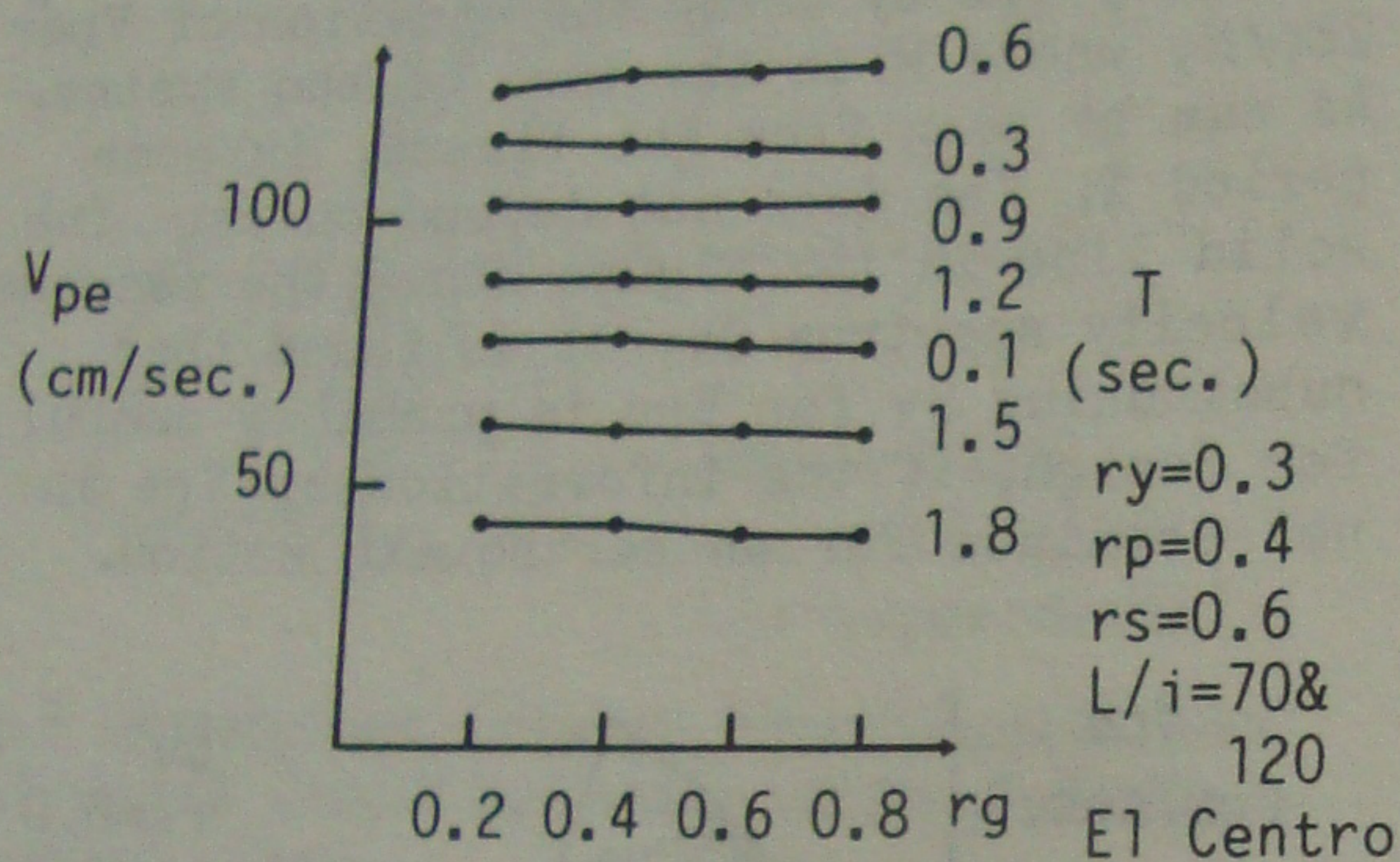


Fig.12 V_{pe} - r_g relation using T

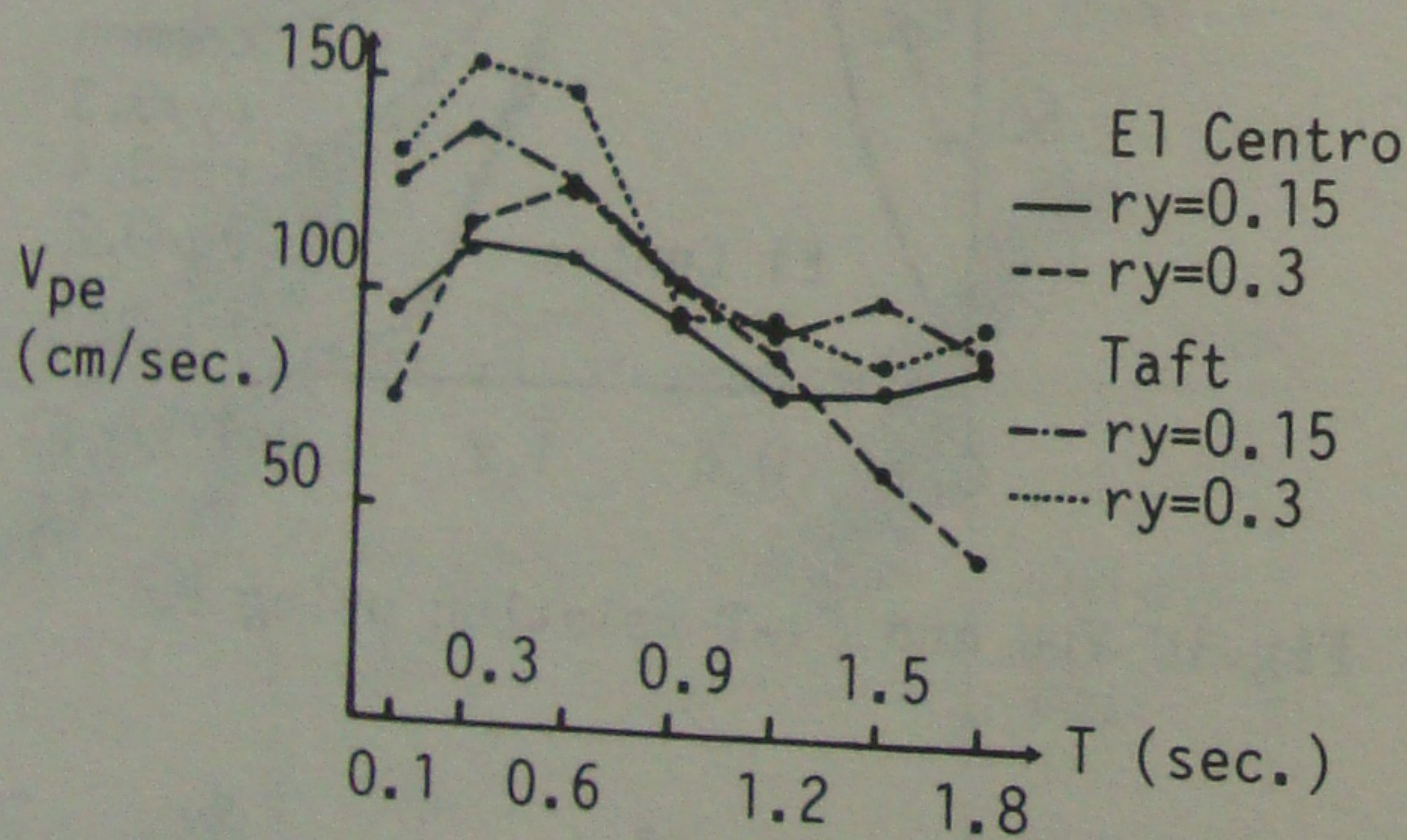


Fig.13 V_{pe} - T relation for r_y and earthquake motion

-plastic-strain-energy shared by braces-
The ratio R_b of plastic-strain-energy dissipated in the braces to the total plastic-strain-energy absorbed in the system was investigated to attain knowledge on allocation of the energy shared by the K-braced portion and the moment-resisting frame portion. The relation between R_b and r_s is shown in Fig.14 for the case

$r_s=r_p+0.1$, associated with T . When $r_s=r_p$, the story displacement at the brace-buckling is equal to that at the initiation of the moment-frame yielding in the assumed model. From Fig.14, first, R_b increases in accordance with the increase of r_s ; second, the manner of increasing of R_b somewhat depends upon T .

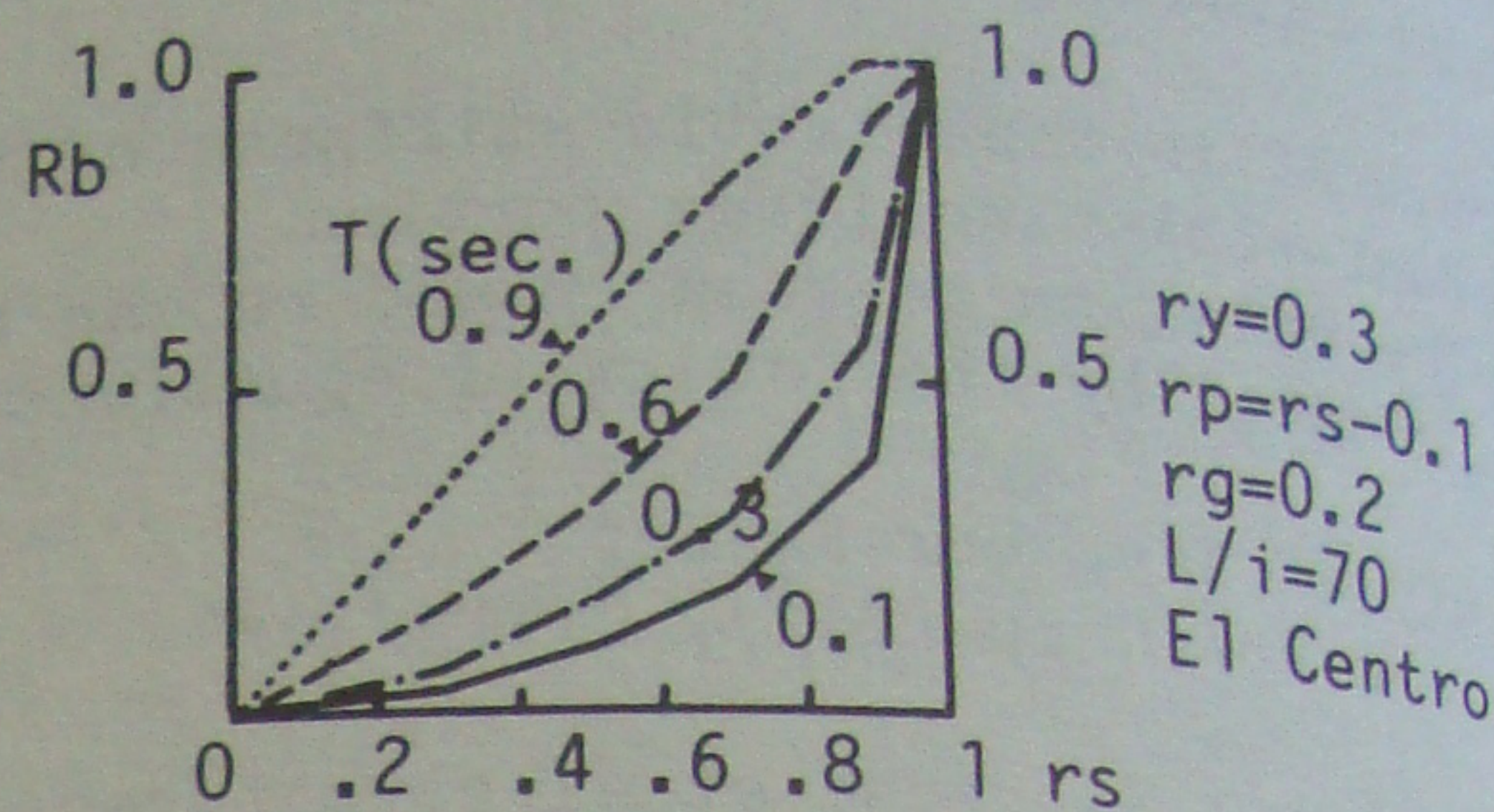


Fig.14 R_b - r_s relation for T

-Plastic-strain-energy absorbed in the compression-side of the brace hysteresis-
The plastic-strain-energy absorbed in the brace consists of the plastic-energy absorbed in the compression-side and in the tension-side (Fig.7). Here, the ratio of the compression-side energy of one brace to the gross plastic-strain-energy of the K-braced portion is defined as R_{bc} . In any combination among r_y , r_p , r_g , r_s and T exclusive of the case $r_p=r_s$ and $T=0.9$, R_{bc} maintains almost 0.3 (Fig.15). In the case $r_p=r_s$ and $T=0.9$, the response displacements of the system have a lot of drift to one direction, resulting in much concentration of the plastic-energy into one-side brace.

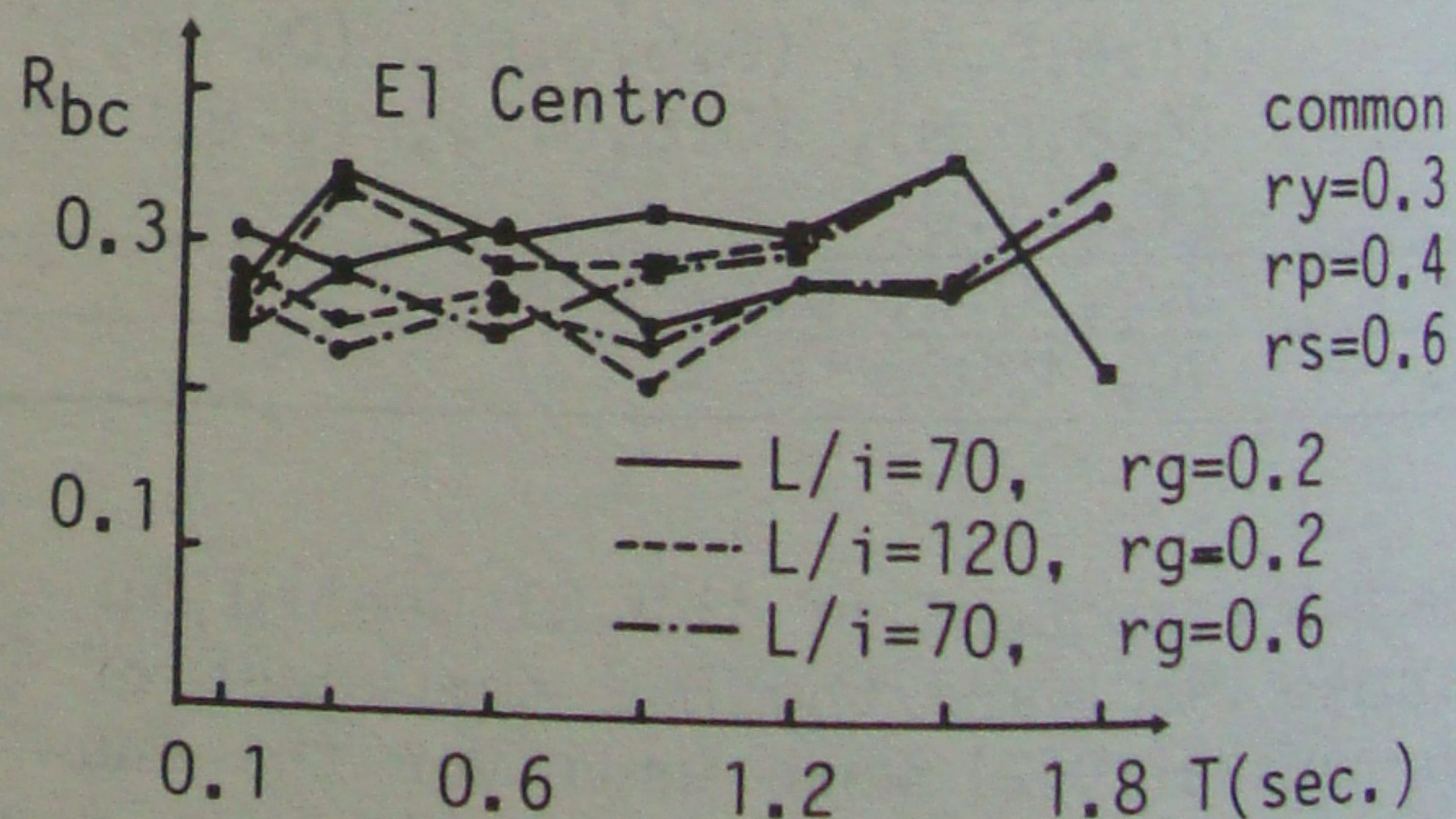


Fig.15 R_{bc} - T relation

-Plastic-strain-energy absorbed in the tension-side of the brace hysteresis-
For one bracing member in the K-braced portion, the plastic-strain-energy absorbed in the tension-side is divided into the energy absorbed in the tension-side skeleton-part and in the transit part up to the skeleton part in the hysteresis model

(Fig.7). Herein, the ratio of the plastic-energy corresponding to the skeleton-part to the gross plastic-energy absorbed in the K-braced portion is defined as R_{bs} . The influence of L/i and rg on R_{bs} corresponding to each brace of K-braced portion is visible in Fig.16 as a function of T . Here, the bold line denotes the mean value of R_{bs} between the two braces. Judging from the figure, R_{bs} does not depend on L/i and rg , and the mean value of R_{bs} between the two braces is stable for T and is at most 0.2. On the contrary, R_{bs} varies by r_y , r_p , r_s and the earthquake motions.

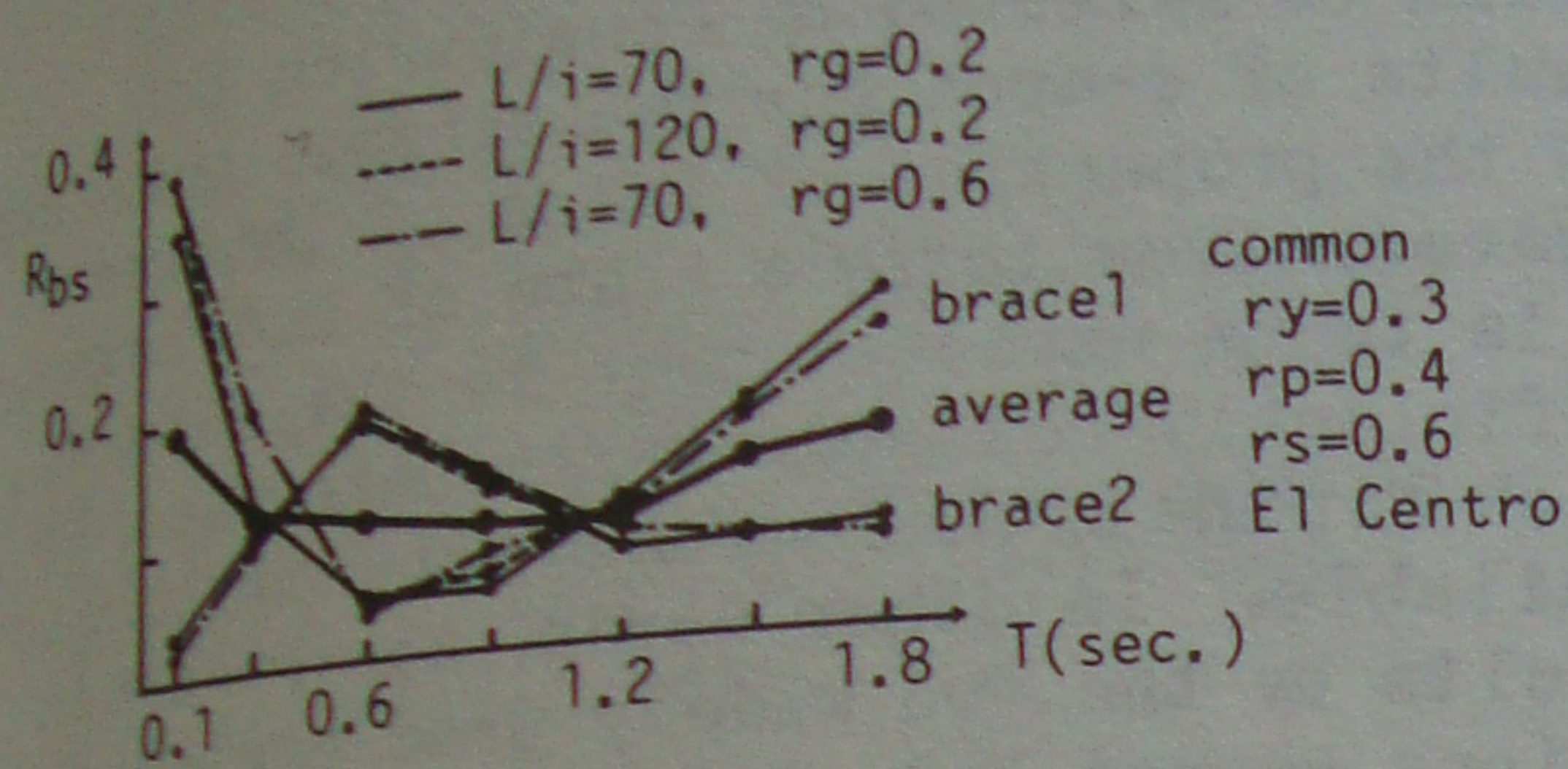


Fig.16 R_{bs} - T relation

3.3 Examinations on analytical results on three-mass system

To confirm the knowledge gained up to the previous sections for multi-story K-braced structures, a series of response analyses on three-degree-of-freedom dynamic systems with the proposed hysteresis model were carried out. The structural parameters and variables used are listed in Table 2. As a conclusion, the knowledge attained for the one-mass system was confirmed again for the multi-mass systems (Figs.17, 18 and 19).

Table 2 Parameters used in analysis of three-mass system

story	M_i/M	K_i/K	r_{yi}/r_y	rg	L/i
1	1.0	1.0	0.15	0.2	70
2	1.0	2/3	0.15 A_2	0.2	70
3	1.0	1/3	0.15 A_3	0.2	70

$T=(0.1, 0.3, 0.6, 0.9, 1.2, 1.5, 1.8)$
 $r_p=r_s=(0.2, 0.4, 0.6, 0.8, 1.0)$, which are specified for each story, respectively.
 $A_2=1+1.12T/(1+3T)$, $A_3=1+2.80T/(1+3T)$

M_i : mass of the i -th story
 K_i : story-stiffness of the i -th story

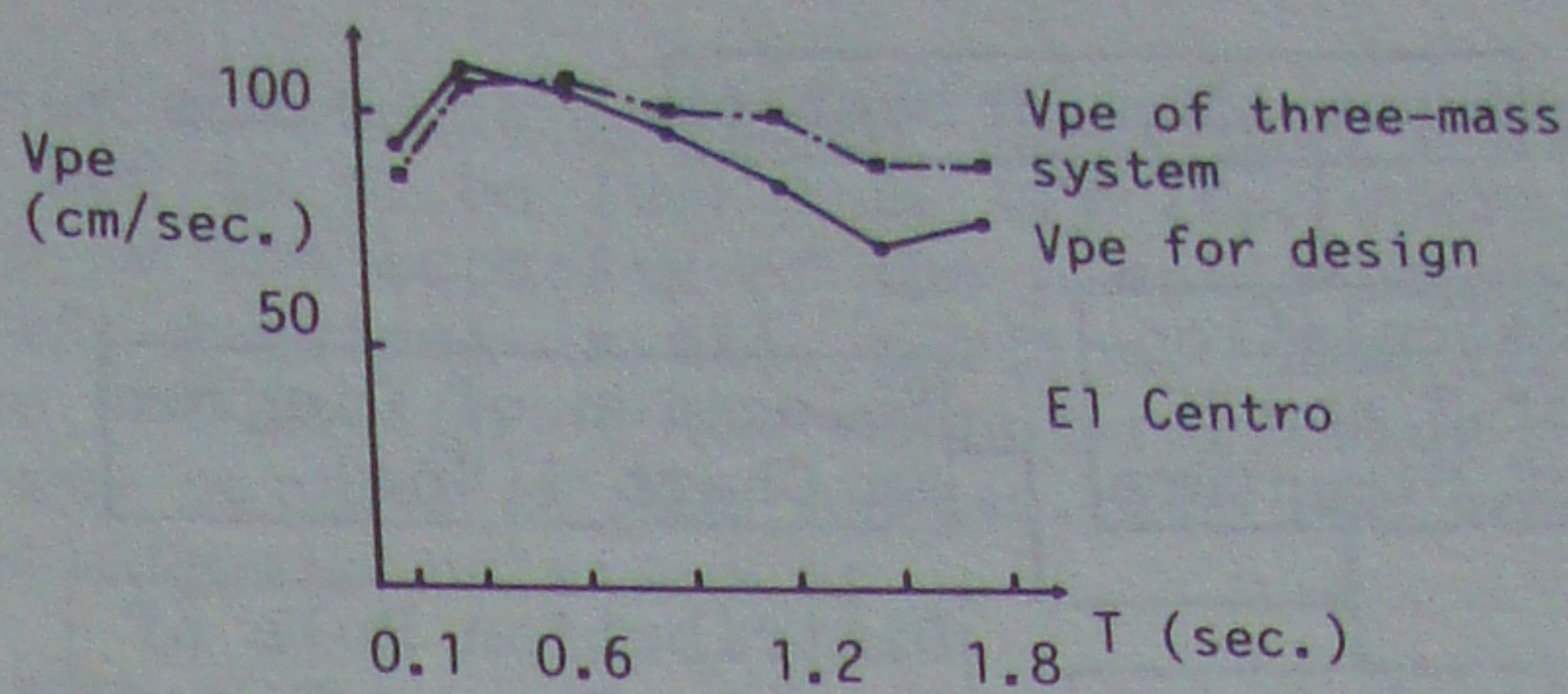


Fig.17 V_{pe} of three-mass system and V_{pe} for design (Chapter 4)

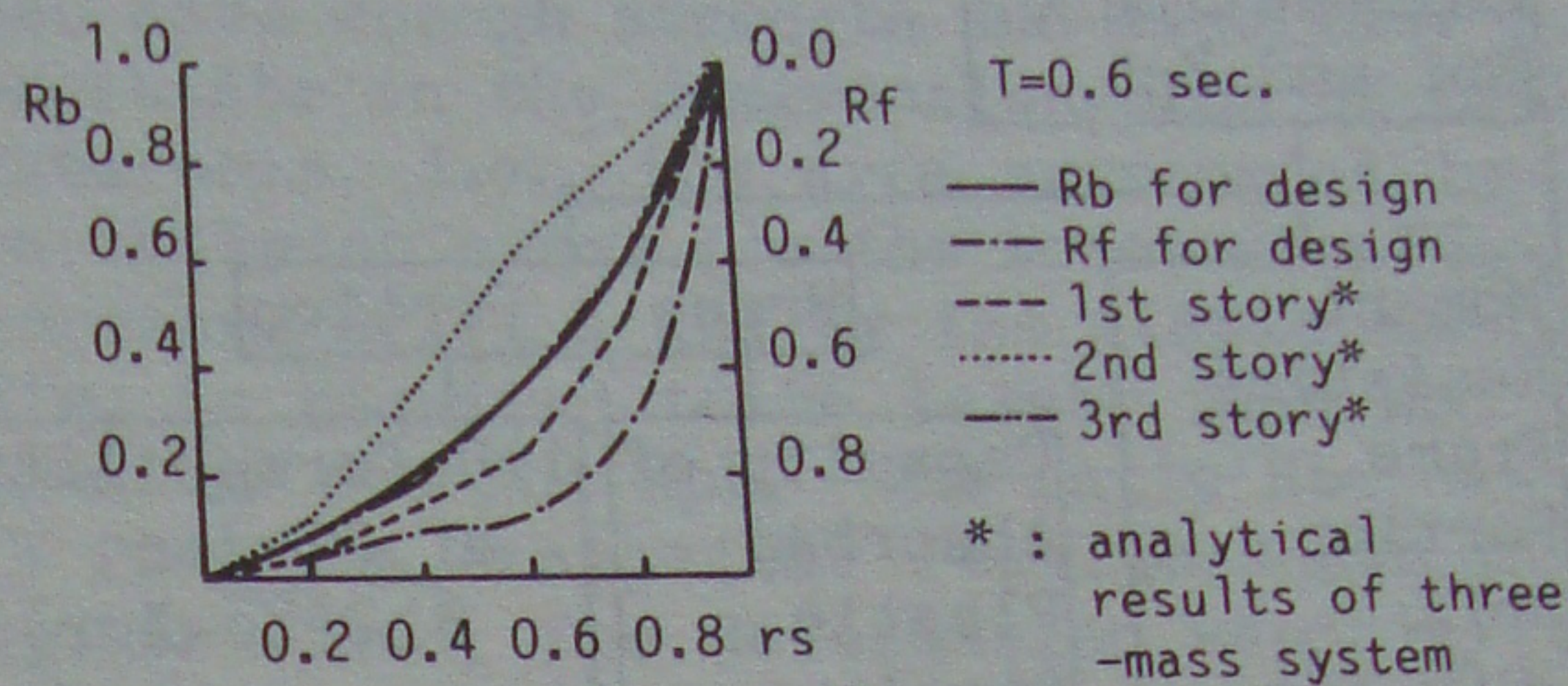


Fig.18 R_b of three-mass system

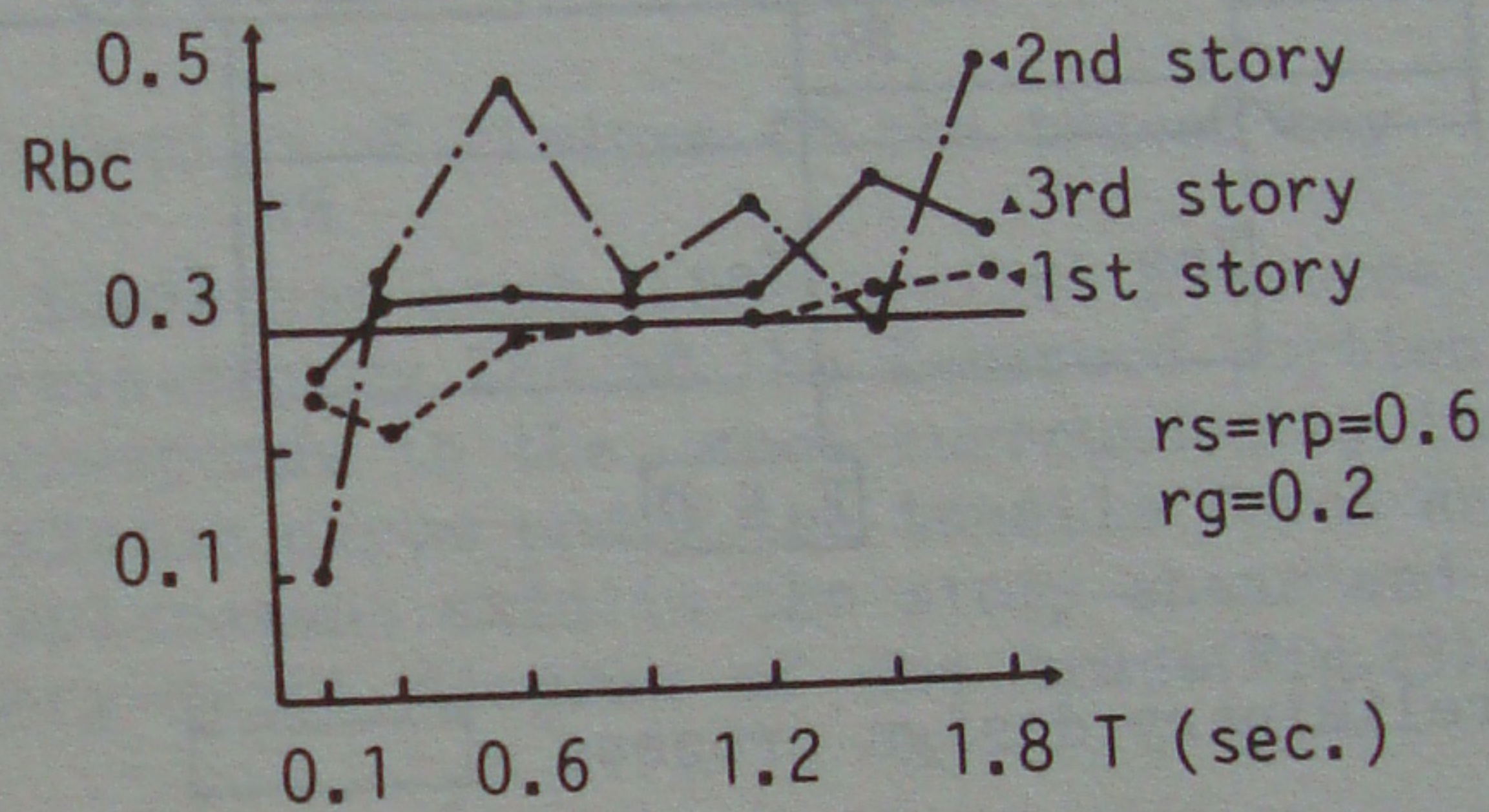


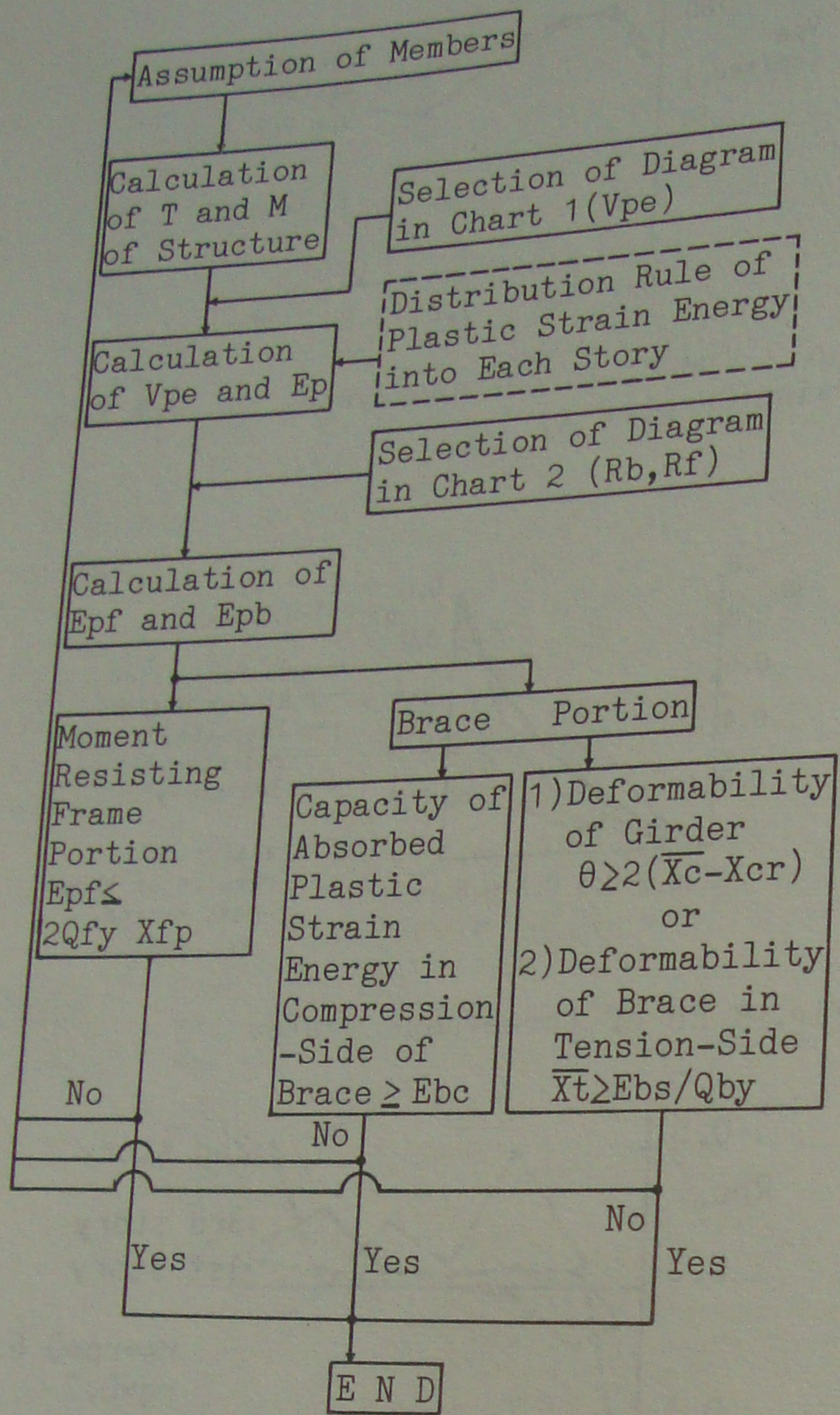
Fig.19 R_{bc} of three-mass-system

4 PROPOSED DESIGN PROCEDURES

Finally, a structural design process for the K-braced system against severe earthquake ground motions is proposed on the basis of the discussions in the previous chapters by the concept on the absorbed plastic-strain-energy into the dynamic system. The outline of the design process is shown in Fig.20 as a block diagram.

4.1 Total strain-energy and its allocation

The equivalent velocity V_{pe} for the design of the K-braced system is given by Chart 1 in Fig.21. According to the consideration



preliminary design process
 proposed design process

Fig.20 Block diagram for design of K-braced steel structure

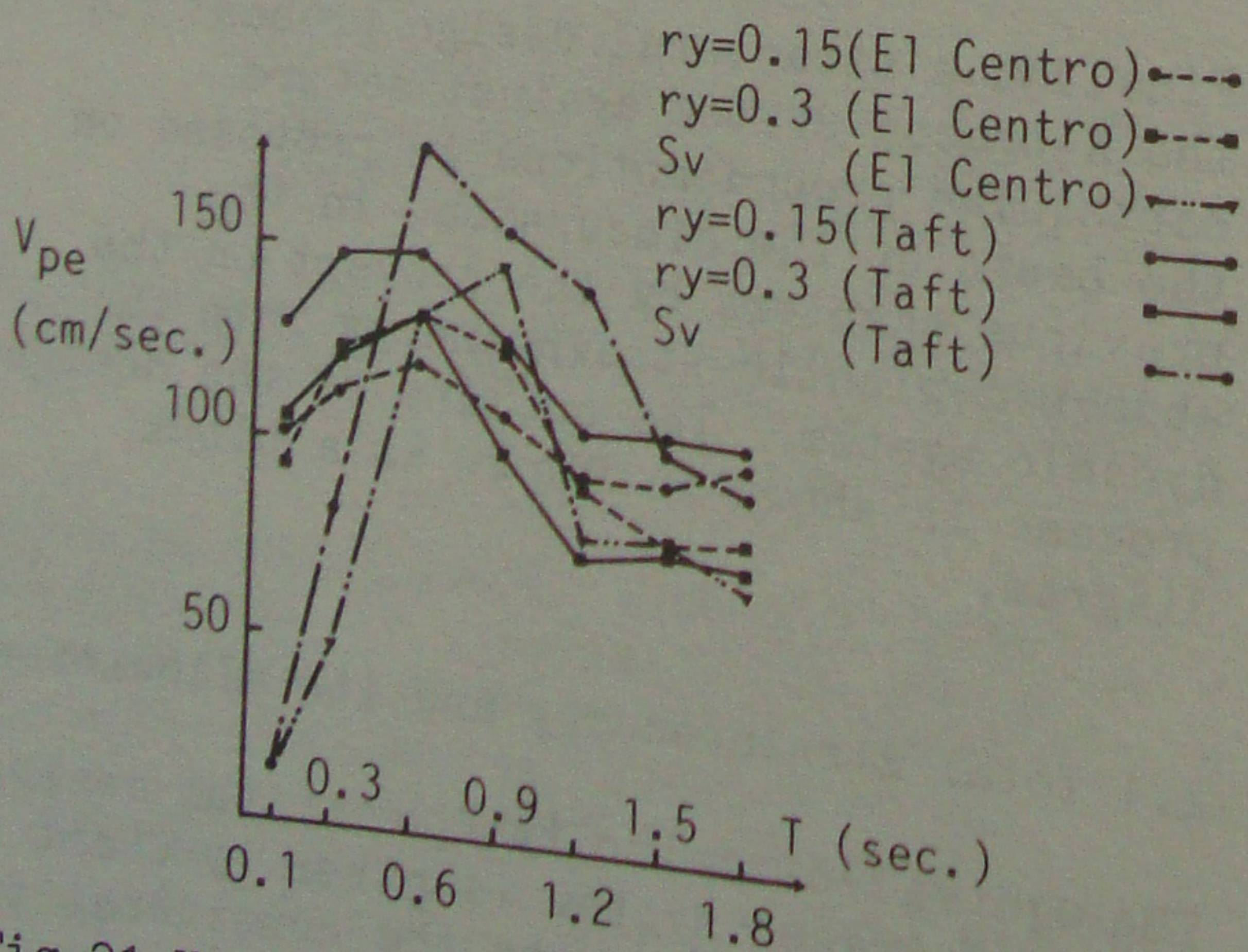


Fig.21 Vpe for design (Chart 1)

on V_{pe} in Chapter 3, V_{pe} does not depend on L/i of braces and the contribution-factor r_g of girders. On the other hand, neat relation among r_s , r_p and V_{pe} have not been always found out, so that the recommendable values of V_{pe} have to be given by taking the scattering response by r_s and r_p into account. From this point of view, Chart 1 in Fig.21 provides the curves of V_{pe} as a function of T just enveloping the scattering response due to r_s and r_p , for both the strength level r_y and the used earthquake records.

The V_{pe} recommended in Chart 1 is, of course, based on the results by the specific records of the past two severe earthquakes. Ideally speaking, earthquake ground motions adopted for the design should be selected by considering the results of search for the seismic activity and the properties of sites of interest. However, from today's state of knowledge, it is to be expected that in the future, sufficiently reliable earthquake records which fit the situation encountered will be available. In other words, the response results by the two widely used earthquake motions cannot help being judged as the next best index for engineering-design aspects.

Now, the total plastic-strain-energy E_{pi} absorbed in the i -th story for a multi-story building structure is given by the following equation.

$$E_{pi} = (M V_{pe}^2 / 2) D_i \quad (14)$$

where M is the total mass of the building, and D_i is the distribution coefficient of the absorbed plastic-strain-energy for the i -th story of the building, for instance, which was vigorously investigated by Akiyama(1985). By his investigation, the coefficient D_i is very sensitively varied by the deviation of the actual story-strength (r_y) from an optimum story-strength proportion that would be able to share response plastic-energy almost equally with every story. Also D_i would be considerably influenced by unknown characteristics of earthquake ground motion (Yamanouchi 1985).

Assuming the coefficient D_i that was developed by Akiyama, the plastic-energy E_{pi} by Eq.14 has to be, for the next step of the design, divided into the two sub-structures, i.e., the moment-resisting frame portion and K-braced portion, by using the distribution ratios, R_f and R_b given by Chart 2 in Fig.22. For the two ratios given, the energy allocated for the two sub-structural systems is obtained respectively as

$$E_{pf} = R_f E_{pi}, E_{pb} = R_b E_{pi} \quad (15)$$

where E_{pf} and E_{pb} are for the moment-resisting frame portion and for the K-braced portion, respectively.

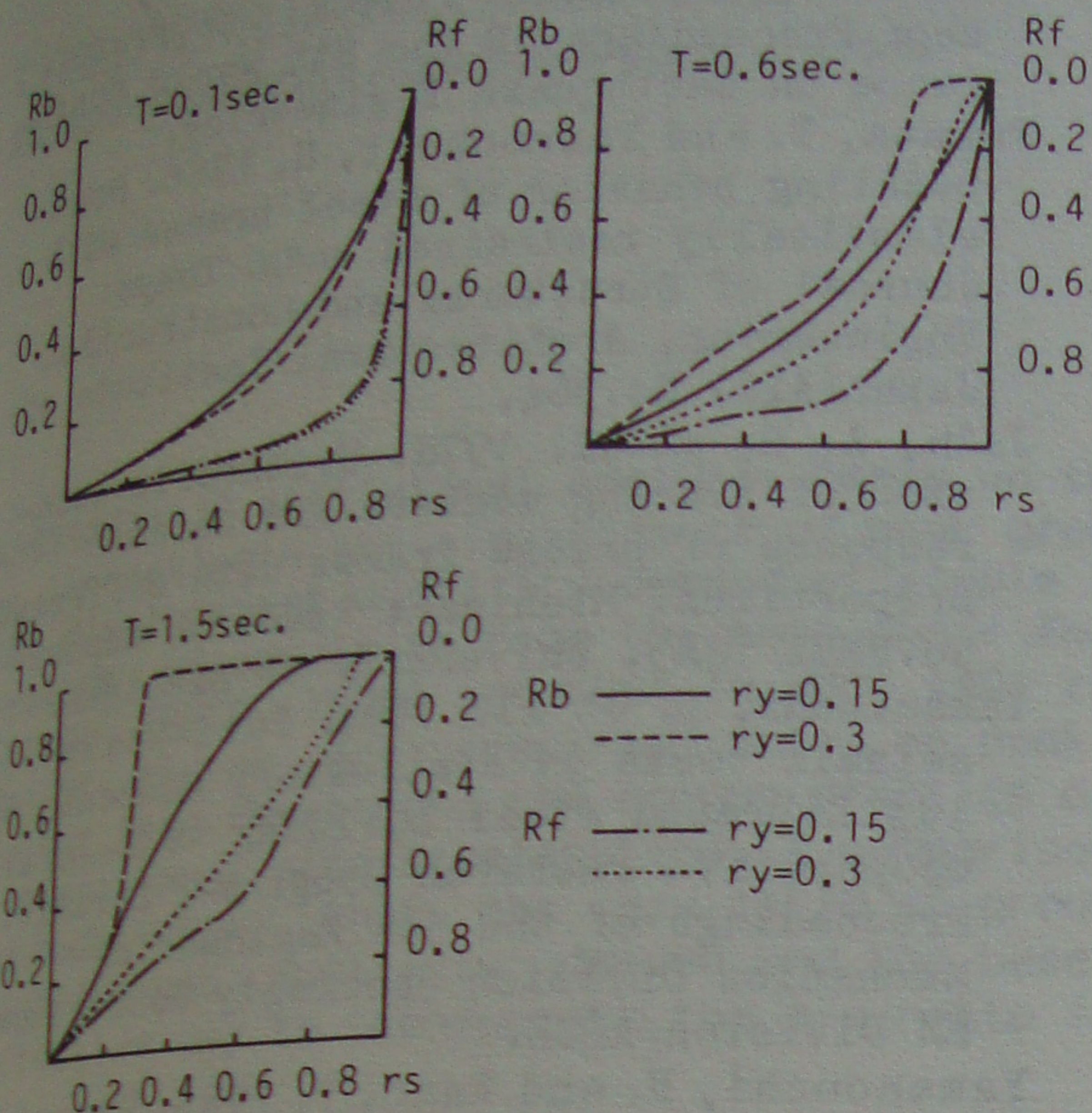


Fig.22 R_f and R_b for design (Chart 2)

As is discussed in Chapter 3, R_b does not depend on the values of L/i and r_g . Considering the uncertainty of earthquakes during the life-time of buildings, properties of the earthquakes have few effect on the values of R_b . Therefore, R_b in Chart 2 is prepared for the design of the K-braced portion in terms of r_s , r_y and T . Moreover R_b is conservatively shown as the maximum in the response of the analyzed one-mass system. And R_f -values in the chart are prepared for the design of the moment-resisting frame portion and has the same meaning as the case for R_b -values.

4.3 Design of moment-resisting frame portion

The moment-resisting frame portion should have enough strength and ductility to absorb the plastic-strain-energy E_{pf} . In general, a structure under a strong ground motion tends to exhibit almost identical response in both positive and negative horizontal directions. Further, as was investigated by Akiyama(1985), the sum of the plastic-strain-energy under the cyclic loading corresponds to the plastic-strain-energy surrounded by the skeleton curve

under monotonic loading. Therefore, a half of E_{pf} is to be less than $Q_f y \bar{X}_{fp}$, where \bar{X}_{fp} is the capacity of the plastic story-drift required in this portion. Namely, for the design of the moment-resisting frame portion of the system, \bar{X}_{fp} has to satisfy the relation of

$$\bar{X}_{fp} \geq E_{pf} / (2Q_f y) \quad (16)$$

4.4 Design of braces

The braces in the K-braced portion should also have enough strength and ductility to absorb E_{bc} in the compression-side of their hysteresis, i.e., the area surrounded by the skeleton curve for the monotonically increased drift X and by the displacement axis, is required to be larger than E_{bc} given by $E_{bc} = R_{bc} E_{pb}$. The ratio R_{bc} can be 0.3 from the analytical results shown in Fig.15. Thus, the deformation capacity of the braces in the compression-side can be obtained from the compression-side skeleton curve and be compared with the required displacement based on E_{bc} .

4.5 Design of girders in the braced bay

On the other hand, the required plastic-strain-energy E_{bs} of the K-braced portion corresponds to the area surrounded by the skeleton curve under the tensile force and displacement axis in the story-shear and story-drift diagram of the brace(Fig.23).

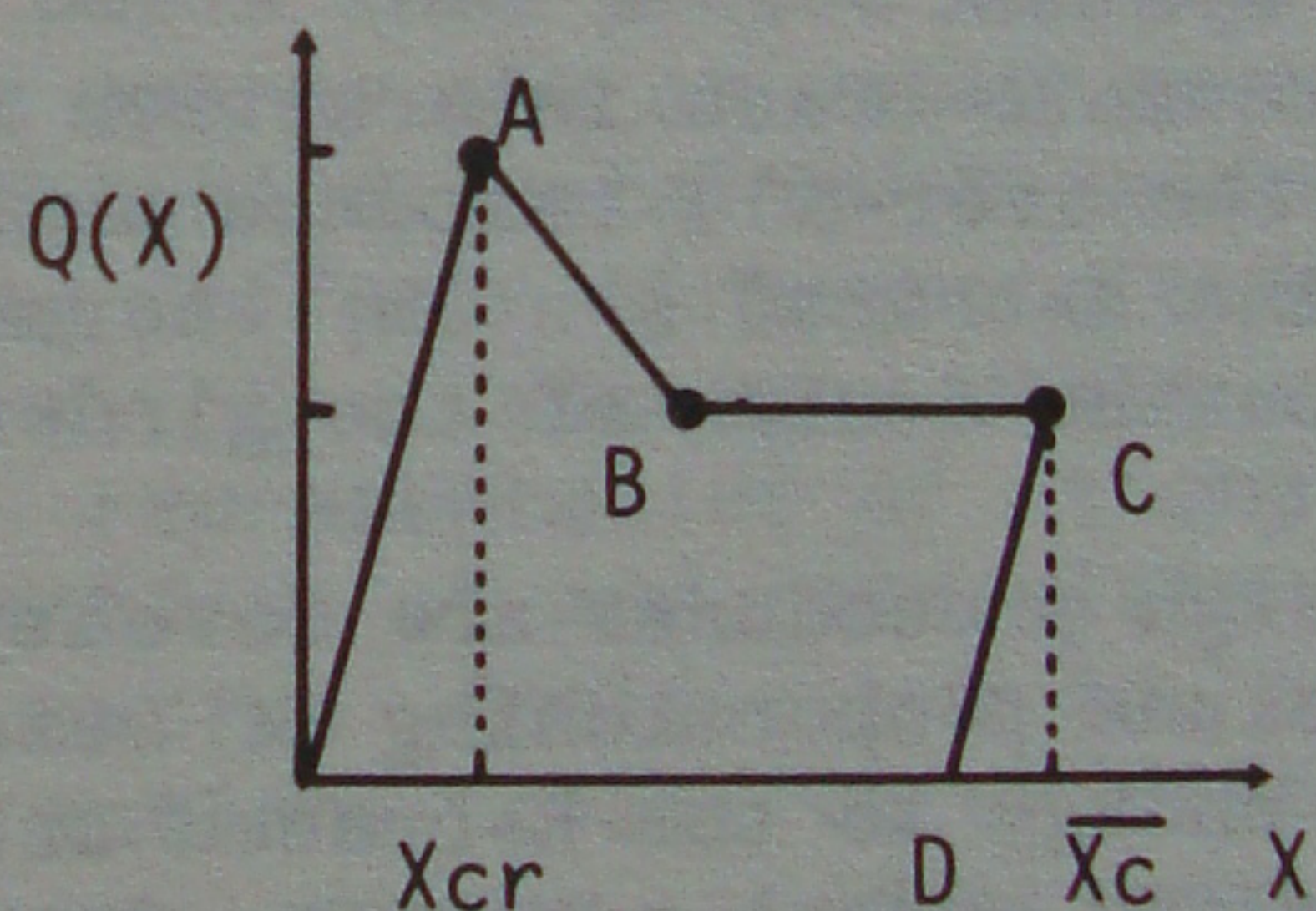


Fig.23 E_{bs} and \bar{X}_c of girder in braced bay

Considering that the area $O-A-B-C-D-O$ is required to be equal to E_{bs} for design, the story drift \bar{X}_c is obtained. Actually, the plastic-strain-energy, corresponding to this area, is absorbed in the girder of the braced bay. It is because that the brace in the K-braced system seldom yields in tension as described in Chapter 2. The girder of the braced bay is, therefore, required to rotate at its mid-span more than the angle given by the following equation.

$$\theta = 2(\bar{X}_c - X_{cr}) / h \quad (17)$$

where X_{cr} is the story displacement at the buckling of the brace and h is the story height. As is described in Chapter 3, R_{bs} does not depend on L/i and r_g . Moreover, considering simplicity of the design and uncertainty of earthquakes, it is reasonable to simplify the relation between R_{bs} and the other parameters. Namely though R_{bs} varies from 0.0 to 0.4 for these parameters, the average value of R_{bs} in a pair of K-braces is at most 0.2 in Fig.16. Therefore, R_{bs} in practical design can take 0.2, i.e., E_{bs} can be equal to 20% of E_{pb} .

In spite of the above discussions, if the girder in the braced bay is so strong as $Q_{gmax} > Q_{by} - Q_{uc}$ (see Fig.5), the energy E_{bs} has to be born by the brace in tension-side. Therefore, the axial deformation capacity \bar{X}_t required for the brace in tension is

$$\bar{X}_t \geq E_{bs} / Q_{by} \quad (18)$$

5 CONCLUSIONS

Through the simple dynamic response analyses on the K-braced structure systems as well as the rational experimental verification, the conclusions can be led to:

The proposed hysteresis model for K-braced systems is simple but reasonable to predict the dynamic behavior of the structure systems.

The interaction between girders in the K-braced bays and braces is clearly introduced into the hysteresis rule of the K-braced system.

The girder-to-brace interaction is not prime in the over-all response characteristics of the K-braced system, whereas it affects on the design of the girders and braces.

The design procedures are developed, which include proportioning of seismic response energy to the K-braced sub-structure and moment-resisting frame sub-structure.

ACKNOWLEDGEMENTS

The authors heartily express thanks for Prof. B. Kato and Associated Prof. H. Akiyama of University of Tokyo for their kind advice. Also the authors would sincerely like to thank Mr S. Yasuda, visiting research staff of BRI, for his dedicated help and important suggestions in preparing the manuscript.

REFERENCES

- Akiyama, H. 1985. Earthquake-resistant limit-state design for buildings. Tokyo: University of Tokyo Press.
- Fukuta, T., Yamanouchi, H. et al. 1984. Hysteresis behavior of three story concentric K-braced frames. San Francisco: Proceedings of the 8th World Conference on Earthquake Engineering.
- Fukuta, T. and Yamanouchi, H. 1986. Post-buckling behavior of steel braces with elastically restrained ends. Tokyo: Journal of Structural and Construction Engineering, Architectural Institute of Japan(AIJ) No.364.
- Jain, A. K. et al. 1978. Hysteresis behavior of bracing members and seismic response of braced frames with different proportions. Michigan: Research Report No.UMEE 78R3, University of Michigan.
- Yamanouchi, H. et al. 1984. Full-scale seismic tests on a six-story concentric K-braced steel building -U.S.-Japan cooperative research program-. Laramie: Proceedings of the 5th Engineering Mechanics Division Specialty Conference, EM Division/ASCE.
- Yamanouchi, H. and Endo, T. 1985. Dynamic response energy of structures with different weight and rigidity along the height. Nagoya: Proceedings of Annual Conference of AIJ.(in Japanese)